Synthesis, Properties, and X-ray Structures of the Lanthanide η^6-Arene-Bridged Aryloxide Dimers $Ln_2(O\text{-}2,6\text{-}i\text{-}Pr_2C_6H_3)_6$ and Their Lewis Base Adducts $Ln(O\text{-}2,6\text{-}i\text{-}Pr_2C_6H_3)_3(THF)_2$ (Ln = Pr, Nd, Sm, Gd, Er, Yb, Lu)

David M. Barnhart,[1a] David L. Clark,*,[1b] John C. Gordon,[1c] John C. Huffman,[1d] Rebecca L. Vincent,[1c] John G. Watkin,*,[1c] and Bill D. Zwick[1e]

Inorganic, Structural and Applied Chemistry Group (CST-3) and Actinide Materials Chemistry Group (NMT-6), Los Alamos National Laboratory, Los Alamos, New Mexico 87545, and The Molecular Structure Center, Indiana University, Bloomington, Indiana 47405

Received February 11, 1994®

Reaction of 3 equiv of 2,6-diisopropylphenol with $Ln[N(SiMe_3)_2]_3$ (Ln = Nd, Sm, Er) in refluxing toluene and subsequent crystallization yield pale blue (Nd), deep yellow (Sm), or light pink (Er) crystals of the tris(aryloxide) complexes $Ln_2(O\text{-}2,6\text{-}i\text{-}Pr_2C_6H_3)_6$ (Ln = Nd (**1**), Sm (**2**), Er (**3**)) in good yield. X-ray crystallographic studies of **1** and **2** reveal centrosymmetric, dimeric units bridged by η^6-π-arene interactions of a unique aryloxide ligand. Ln–O bond lengths average 2.122(9) (**1**, Nd) and 2.101(6) Å (**2**, Sm) for terminal ligands and 2.211(8) (**1**) and 2.198(5) Å (**2**) for bridging aryloxide ligands. η^6-Arene bridges hold the dimeric units together with an average Ln–C distance of 3.035 Å for **1** and 2.986 and 3.016 Å for the two independent molecules in the asymmetric unit of **2**. Compounds **1**-**3** react with THF in toluene solution to give the THF bisadducts $Ln(O\text{-}2,6\text{-}i\text{-}Pr_2C_6H_3)_3(THF)_2$ (Ln = Nd (**4**), Sm (**5**), Er (**6**)) in essentially quantitative yield. In a related fashion, $Lu(O\text{-}2,6\text{-}i\text{-}Pr_2C_6H_3)_3(THF)_2$ (**7**) was prepared following the reaction of $Lu[N(SiMe_3)_2]_3$ with 3 equiv of diisopropylphenol in the presence of THF. The anhydrous trichlorides of Sm, Pr, Gd, and Yb react with 3 equiv of potassium 2,6-diisopropylphenoxide in THF solution to give the 5-coordinate THF bisadducts $Ln(O\text{-}2,6\text{-}i\text{-}Pr_2C_6H_3)_3(THF)_2$ (Ln = Sm (**5**), Pr (**8**), Gd (**9**), Yb (**10**)). X-ray crystal structures have been obtained for $Ln(O\text{-}2,6\text{-}i\text{-}Pr_2C_6H_3)_3(THF)_2$ (Ln = Er (**6**), Lu (**7**), Pr (**8**), Gd (**9**)). The four compounds are isostructural, and the molecular structure consists of a distorted trigonal bipyramidal lanthanide metal center with two axial THF and three equatorial aryloxide ligands. Ln–O distances for the aryloxide ligands average 2.078 (**6**, Er), 2.044 (**7**, Lu), 2.172 (**8**, Pr), and 2.130 (**9**, Gd) while Ln–O distances for the THF ligands average 2.346 (**6**), 2.296 (**7**), 2.482 (**8**), and 2.394 Å (**9**). Solution ^1H and ^{13}C NMR data, together with solution IR data, strongly support the proposal that the π-arene-bridged dimeric structures of **1**-**3** are maintained in both benzene and toluene solutions at room temperature. Crystal data for **1** (at –162 °C): monoclinic space group $P2_1/a$, a = 9.536(2) Å, b = 21.219(6) Å, c = 17.162(5) Å, β = 104.43(1)°, V = 3363.0 Å^3, Z = 2, d_{calc} = 1.335 g cm^{-3}, $R(F)$ = 0.0518, $R_w(F)$ = 0.0522. Crystal data for **2** (at –70 °C): monoclinic space group $P2_1/c$, a = 9.555(2) Å, b = 21.301(2) Å, c = 33.220(4) Å, β = 91.50(3)°, V = 6759 Å^3, Z = 2 (2 molecules per asymmetric unit), d_{calc} = 1.341 g cm^{-3}, $R(F)$ = 0.0447, $R_w(F)$ = 0.0640. Crystal data for **6** (at –170 °C): monoclinic space group $P2_1$, a = 9.693(1) Å, b = 19.141(3) Å, c = 12.083(1) Å, β = 109.48(1)°, V = 2113.50 Å^3, d_{calc} = 1.325 g cm^{-3}, Z = 2, $R(F)$ = 0.047, $R_w(F)$ = 0.063. Crystal data for **7** (at –70 °C): monoclinic space group $P2_1$, a = 9.632(1) Å, b = 19.269(2) Å, c = 12.164(1) Å, β = 109.52(1)°, V = 2127.9 Å^3, d_{calc} = 1.328 g cm^{-3}, Z = 2, $R(F)$ = 0.021, $R_w(F)$ = 0.031. Crystal data for **8** (at –70 °C): monoclinic space group $P2_1$, a = 9.857(2) Å, b = 19.408(4) Å, c = 12.085(3) Å, β = 109.81(2)°, V = 2175.1 Å^3, d_{calc} = 1.247 g cm^{-3}, Z = 2, $R(F)$ = 0.045, $R_w(F)$ = 0.061. Crystal data for **9** (at –70 °C): monoclinic space group $P2_1$, a = 9.755(1) Å, b = 19.377(2) Å, c = 12.184(1) Å, β = 109.65(1)°, V = 2168.1 Å^3, d_{calc} = 1.276 g cm^{-3}, Z = 2, $R(F)$ = 0.054, $R_w(F)$ = 0.073.

Introduction

The alkoxide and aryloxide chemistry of scandium, yttrium, and the lanthanide elements is the subject of considerable current interest, with a wide range of structural types being documented in recent years.[2–23] In the case of aryloxide complexes, a great deal of control upon the coordination number and degree of oligomerization of the products is available through the use of

® Abstract published in *Advance ACS Abstracts*, July 1, 1994.

(1) (a) CST-3. Present address: Department of Chemistry, University of Washington, BG-10, Seattle, WA 98185. (b) CST-3, Mail Stop G739. (c) CST-3, Mail Stop C346. (d) Molecular Structure Center, Indiana University. (e) NMT-6, Mail Stop E510.

(2) Bradley, D. C.; Chudzynska, H.; Hursthouse, M. B.; Motevalli, M. *Polyhedron* **1991**, *10*, 1049.
(3) Evans, W. J.; Golden, R. E.; Ziller, J. W. *Inorg. Chem.* **1991**, *30*, 4963.
(4) Hitchcock, P. B.; Lappert, M. F.; MacKinnon, I. A. *J. Chem. Soc., Chem. Commun.* **1988**, 1557.
(5) Coan, P. S.; McGeary, M. J.; Lobkovsky, E. B.; Caulton, K. G. *Inorg. Chem.* **1991**, *30*, 3570.
(6) McGeary, M. J.; Coan, P. S.; Folting, K.; Streib, W. E.; Caulton, K. G. *Inorg. Chem.* **1991**, *30*, 1723.
(7) Evans, W. J.; Deming, T. J.; Olofson, J. M.; Ziller, J. W. *Inorg. Chem.* **1989**, *28*, 4027.
(8) Poncelet, O.; Hubert-Pfalzgraf, L. G. *Polyhedron* **1989**, *8*, 2183.
(9) Schumann, H.; Kociok-Köhn, G.; Loebel, J. *Z. Anorg. Allg. Chem.* **1990**, *581*, 69.
(10) Helgesson, G.; Jagner, S.; Poncelet, O.; Hubert-Pfalzgraf, L. G. *Polyhedron* **1991**, *10*, 1559.
(11) Caulton, K. G.; Hubert-Pfalzgraf, L. G. *Chem. Rev.* **1990**, *90*, 969.
(12) Mehrotra, R. C.; Singh A.; Tripathi, U. M. *Chem. Rev.* **1991**, *91*, 1287.
(13) (a) Stecher, H. A.; Sen, A.; Rheingold, A. *Inorg. Chem.* **1988**, *27*, 1130. (b) Sen, A.; Stecher, H. A.; Rheingold, A. *Inorg. Chem.* **1992**, *31*, 473.
(14) Deacon, G. B.; Hitchcock, P. B.; Holmes, S. A.; Lappert, M. F.; MacKinnon, P.; Newnham, R. H. *J. Chem. Soc., Chem. Commun.* **1989**, 935.
(15) Lappert, M. F.; Singh, A.; Smith, R. G. *Inorg. Synth.* **1990**, *27*, 164.
(16) Poncelet, O.; Sartain, O. W. J.; Hubert-Pfalzgraf, L. G.; Folting, K.; Caulton, K. G. *Inorg. Chem.* **1989**, *28*, 263.
(17) Livage, J.; Henry, M.; Sanchez, C. *Prog. Solid State Chem.* **1988**, *18*, 259.
(18) Sasai, H.; Suzuki, T.; Arai, S.; Arai, T.; Shibasaki, M. *J. Am. Chem. Soc.* **1992**, *114*, 4418.
(19) Clark, D. L.; Huffman, J. C.; Watkin, J. G. *Inorg. Chem.* **1992**, *31*, 1554.
(20) Sasai, H.; Suzuki, T.; Arai, S.; Arai, T.; Shibasaki, M. *J. Am. Chem. Soc.* **1992**, *114*, 4418.

0020-1669/94/1333-3487$04.50/0

bulky substituents on the arene ring. This strategy has produced complexes exhibiting a number of interesting structural types, involving 2,6-dimethylphenoxide,[24] 2,6-diphenylphenoxide,[25] 2,6-di-*tert*-butylphenoxide,[26–28] 4-methylphenoxide,[29] and binaphtholate[30] ligation. It is known, for example, that the metathesis reaction of $LnCl_3$ (Ln = lanthanide metal) with 3 equiv of the sterically demanding lithium aryloxide LiO-2,6-*t*-Bu_2-4-MeC_6H_2, leads to the formation of mononuclear $Ln(OAr)_3$ complexes for the whole of the lanthanide series.[26] In some cases these compounds will accept 1 or 2 equiv of Lewis base to form adducts of general formula $Ln(O\text{-}2,6\text{-}t\text{-}Bu_2C_6H_3)_3(L)_n$ (n = 1, 2).[13a,26] The use of the less sterically demanding 2,6-dimethylphenoxide ligand produces, in the case of yttrium, the THF trisadduct $Y(O\text{-}2,6\text{-}Me_2C_6H_3)_3(THF)_3$, which loses THF upon crystallization from toluene to yield dimeric $Y_2(O\text{-}2,6\text{-}Me_2C_6H_3)_6(THF)_4$.[24] Employing aryloxide ligands with no substitution in the 2,6-positions can lead to the isolation of heterometallic lanthanide clusters such as $Na_3La_2(O\text{-}4\text{-}MeC_6H_4)_9(THF)_5$.[29]

The amount of structural data available for homoleptic Sc, Y, or lanthanide aryloxide complexes in the absence of a Lewis base is fairly limited, being confined to just a few examples: 3-coordinate $Sc(O\text{-}2,6\text{-}t\text{-}Bu_2\text{-}4\text{-}MeC_6H_2)_3$[26] and $Ce(O\text{-}2,6\text{-}t\text{-}Bu_2C_6H_3)_3$,[13a] and $Yb(O\text{-}2,6\text{-}Ph_2C_6H_3)_3$,[25] which features an *intra*molecular Yb···π-arene interaction. We and others have shown that 2,6-di-*tert*-butylphenoxide complexes of the early actinide elements (An = U, Th) display different reactivity compared to compounds of the less sterically demanding 2,6-diisopropylphenoxide ligand.[31,32] Therefore we set out to examine the chemistry of the lanthanide elements with moderately bulky 2,6-diisopropylphenoxide ligation; we report here the preparation and structural characterization of homoleptic lanthanide tris(aryloxide) complexes containing this ligand and present evidence for their existence as π-arene-bridged dimeric species both in the solid state *and* in solution. The isolation and characterization of THF bisadducts of the lanthanide aryloxides, employing both metathesis and alcoholysis routes, are also described.

Results and Discussion

Synthesis and Reactivity. The addition of 3 equiv of 2,6-diisopropylphenol to a toluene solution of $Ln[N(SiMe_3)_2]_3$ (Ln = Nd, Sm, Er) followed by 2 h of reflux and subsequent crystallization (–40 °C) from the same solvent yields pale blue (Nd), deep yellow (Sm), or light pink (Er) crystals of the tris(aryloxide) dimers $Ln_2(O\text{-}2,6\text{-}i\text{-}Pr_2C_6H_3)_6$ (Ln = Nd (**1**), Sm (**2**), Er (**3**)) in good yield according to eq 1. Complexes **1-3** are very sparingly soluble in hexane and moderately soluble in benzene and toluene.

$$2Ln[N(SiMe_3)_2]_3 + 6HOAr \xrightarrow[\text{reflux}]{\text{toluene}} Ln_2(OAr)_6 + 6HN(SiMe_3)_2 \quad (1)$$

$$Ln = Nd\ (\mathbf{1}),\ Sm\ (\mathbf{2}),\ Er\ (\mathbf{3});\ Ar = 2,6\text{-}i\text{-}Pr_2C_6H_3$$

$$Ln_2(OAr)_6 + 4THF \xrightarrow{\text{toluene}} 2Ln(OAr)_3(THF)_2 \quad (2)$$

$$Ln = Nd\ (\mathbf{4}),\ Sm\ (\mathbf{5}),\ Er\ (\mathbf{6});\ Ar = 2,6\text{-}i\text{-}Pr_2C_6H_3$$

The addition of a Lewis base such as THF to benzene solutions of **1-3** results in cleavage of the dimeric unit and formation of THF bisadducts $Ln(O\text{-}2,6\text{-}i\text{-}Pr_2C_6H_3)_3(THF)_2$ (Ln = Nd (**4**), Sm (**5**), Er (**6**)) as indicated in eq 2. The cleavage of $Ln_2(OAr)_6$ units with Lewis base to give monomeric $Ln(OAr)_3L_2$ complexes is analogous to that seen in the yttrium aryloxide complex $Y_2(O\text{-}2,6\text{-}Me_2C_6H_3)_6(THF)_2$, which reversibly interconverts between the monomeric trisolvate $Y(O\text{-}2,6\text{-}Me_2C_6H_3)_3(THF)_3$ and dimeric $Y_2(O\text{-}2,6\text{-}Me_2C_6H_3)_6(THF)_2$ in toluene solution.[24] However, the $Ln_2(OAr)_6$ complexes **1-3** are remarkably sensitive to Lewis base. The reaction shown in eq 2 is irreversible, and even small traces of THF in the drybox atmosphere surrounding solid samples of **1-3** will result in substantial amounts of $Ln(OAr)_3(THF)_2$ complexes being formed. This extreme sensitivity and irreversibility of the reaction with Lewis base are remarkably different from those observed with the yttrium complex noted above and with those observed for aliphatic $Nd_2(OR)_6L_2$ compounds which retain their dimeric nature, even in neat solutions of Lewis base (eqs 3 and 4).[33a] This sensitivity is related to the unusual structure of these $Ln_2(OAr)_6$ compounds both in the solid state and in solution (vide infra). The THF bisadduct $Lu(O\text{-}2,6\text{-}i\text{-}Pr_2C_6H_3)_3(THF)_2$ (**7**) was prepared in a one-pot reaction by the interaction of $Lu[N(SiMe_3)_2]_3$ with 3 equiv of $HO\text{-}2,6\text{-}i\text{-}Pr_2C_6H_3$ in refluxing toluene in the presence of THF, as outlined in eq 5.

$$2Nd[N(SiMe_3)_2]_3 \xrightarrow[\text{hexane/THF}]{6HOCH\text{-}i\text{-}Pr_2} Nd_2(OCH\text{-}i\text{-}Pr_2)_6(THF)_2 + 6HN(SiMe_3)_2 \quad (3)$$

$$Nd_2(OCH\text{-}i\text{-}Pr_2)_6(THF)_2 \xrightarrow{\text{pyridine (excess)}} Nd_2(OCH\text{-}i\text{-}Pr_2)_6(py)_2 + 2THF \quad (4)$$

$$Ln[N(SiMe_3)_2]_3 + 3HOAr \xrightarrow[\text{reflux}]{\text{toluene/THF}} Ln(OAr)_3(THF)_2 + 3HN(SiMe_3)_2 \quad (5)$$

$$Ln = Lu\ (\mathbf{7});\ Ar = 2,6\text{-}i\text{-}Pr_2C_6H_3$$

The room-temperature reaction of anhydrous $LnCl_3$ (Ln = Pr, Sm, Gd, Yb) with 3 equiv of potassium 2,6-diisopropylphenoxide in THF, followed by crystallization from toluene, results in the isolation of crystalline, monomeric THF bisadducts $Ln(OAr)_3(THF)_2$ (Ln = Sm (**5**, pale yellow), Pr (**8**, pale brown), Gd (**9**, pale green), Yb (**10**, yellow)) in good yield according to eq 6. However, we also note that the reaction shown in eq 6 is not general to all of the lanthanide trichlorides. Attempts to prepare $Ln(O\text{-}2,6\text{-}i\text{-}Pr_2C_6H_3)_3(THF)_2$ complexes from the reaction of $NdCl_3$ or $ErCl_3$ with 3 equiv of $KO\text{-}2,6\text{-}i\text{-}Pr_2C_6H_3$ in THF produced instead the potassium salts $K[Ln(O\text{-}2,6\text{-}i\text{-}Pr_2C_6H_3)_4]$ (Ln = Nd, Er). Subsequent work has shown that these complexes may be prepared in high yield for a variety of lanthanides according

(21) Schaverien, C. J.; Frijns, J. H. G.; Heeres, H. J.; van den Hende, J. R.; Teuben, J. H.; Spek, A. L. *J. Chem. Soc., Chem. Commun.* **1991**, 642.
(22) Poncelet, O.; Hubert-Pfalzgraf, L. G.; Daran, J.-C.; Astier, R. *J. Chem. Soc., Chem. Commun.* **1989**, 1846.
(23) Herrmann, W. A.; Anwander, R.; Kleine, M.; Scherer, W. *Chem. Ber.* **1992**, *125*, 1971.
(24) Evans, W. J.; Olofson, J. M.; Ziller, J. W. *Inorg. Chem.* **1989**, *28*, 4308.
(25) Deacon, G. B.; Nickel, S.; MacKinnon, P.; Tiekink, E. R. T. *Aust. J. Chem.* **1990**, *43*, 1245.
(26) Hitchcock, P. B.; Lappert, M. F.; Singh, A. *J. Chem. Soc., Chem. Commun.* **1983**, 1499.
(27) Lappert, M. F.; Singh, A.; Atwood, J. L.; Hunter, W. E. *J. Chem. Soc., Chem. Commun.* **1981**, 1191.
(28) Hitchcock, P. B.; Lappert, M. F.; Smith, R. G. *Inorg. Chim. Acta* **1987**, *139*, 183.
(29) Evans, W. J.; Golden, R. E.; Ziller, J. W. *Inorg. Chem.* **1993**, *32*, 3041.
(30) Schaverien, C. J.; Meijboom, N.; Orpen, A. G. *J. Chem. Soc., Chem. Commun.* **1992**, 124.
(31) Berg, J. M.; Clark, D. L.; Huffman, J. C.; Morris, D. E.; Sattelberger, A. P.; Streib, W. E.; Van Der Sluys, W. G.; Watkin, J. G. *J. Am Chem. Soc.* **1992**, *114*, 10811.
(32) Van Der Sluys, W. G.; Burns, C. J.; Huffman, J. C.; Sattelberger, A. P. *J. Am. Chem. Soc.* **1988**, *110*, 5924.
(33) (a) Barnhart, D. M.; Clark, D. L.; Huffman, J. C.; Vincent, R. L.; Watkin, J. G. *Inorg. Chem.* **1993**, *32*, 4077. (b) Barnhart, D. M.; Clark, D. L.; Gordon, J. C.; Huffman, J. C.; Vincent, R. L.; Watkin, J. G.; Zwick, B. D. To be submitted for publication in *Inorg. Chem.*

Table 1. Summary of Crystal Data[a]

	1	2	6	7	8	9
empirical formula	$Nd_2C_{72}H_{102}O_6$	$Sm_2C_{72}H_{102}O_6$	$ErC_{44}H_{67}O_5$	$LuC_{44}H_{67}O_5$	$PrC_{44}H_{67}O_5$	$GdC_{44}H_{67}O_5$
color of crystal	pale blue	pale yellow	pale pink	green-brown	colorless	yellow/pink
crystal dimens, mm³	0.15 × 0.20 × 0.25	0.2 × 0.15 × 0.13	0.25 × 0.25 × 0.25	0.25 × 0.25 × 0.25	0.23 × 0.12 × 0.12	0.30 × 0.24 × 0.20
space group	$P2_1/a$	$P2_1/c$	$P2_1$	$P2_1$	$P2_1$	$P2_1$
a, Å	9.536(2)	9.555(2)	9.693(1)	9.632(1)	9.857(2)	9.755(1)
b, Å	21.219(6)	21.301(2)	19.141(3)	19.269(2)	19.408(4)	19.377(2)
c, Å	17.162(5)	33.220(4)	12.083(1)	12.164(1)	12.085(3)	12.184(1)
β, deg	104.43(1)	91.50(3)	109.48(1)	109.52(1)	109.81(2)	109.65(1)
temp, °C	−162	−70	−170	−70	−70	−70
Z, molecules/unit cell	2	2 (2 molecules/asym unit)	2	2	2	2
V, Å³	3363.0	6759	2113.5	2127.9	2175.1	2168.1
D_{calc}, g cm⁻³	1.335	1.341	1.325	1.328	1.247	1.276
λ(Mo Kα)	0.710 69	0.710 73	0.710 69	0.710 73	0.710 73	0.710 73
fw	1352.07	1364.2	843.27	850.99	816.9	833.2
abs coeff, cm⁻¹	15.782	17.69	20.50	23.60	11.60	15.69
2θ range, deg	6–45	3–45	6–45	2–50	2–50	2–50
no. of measd refls	8418	9752	2857	5143	4202	4226
no. of unique ints	4375	8807	2857	4839	3651	3971
no. of obsd refls	2526 [$F > 2.33\sigma(F)$]	6789 [$F > 4\sigma(F)$]	2857 [$F > 2.33\sigma(F)$]	4581 [$F > 4\sigma(F)$]	3207 [$F > 6\sigma(F)$]	3568 [$F > 4\sigma(F)$]
$R(F)$[b]	0.0518	0.0447	0.047	0.021	0.045	0.054
$R_w(F)$[c]	0.0522	0.0640	0.063	0.031	0.061	0.073
goodness-of-fit	0.900	2.200	4.267	1.20	1.84	1.83

[a] **1** = $[Nd(O\text{-}2,6\text{-}i\text{-}Pr_2C_6H_3)_3]_2$; **2** = $[Sm(O\text{-}2,6\text{-}i\text{-}Pr_2C_6H_3)_3]_2$; **6** = $Er(O\text{-}2,6\text{-}i\text{-}Pr_2C_6H_3)_3(THF)_2$; **7** = $Lu(O\text{-}2,6\text{-}i\text{-}Pr_2C_6H_3)_3(THF)_2$; **8** = $Pr(O\text{-}2,6\text{-}i\text{-}Pr_2C_6H_3)_3(THF)_2$; **9** = $Gd(O\text{-}2,6\text{-}i\text{-}Pr_2C_6H_3)_3(THF)_2$. [b] $R(F) = \sum||F_o| - |F_c|| / \sum|F_o|$. [c] $R_w(F) = [\sum w(|F_o| - |F_c|)^2 / \sum w|F_o|^2]^{1/2}$; $w = 1/\sigma^2(|F_o|)$.

to the stoichiometry shown in eq 7. The structural chemistry and reactivity of these fascinating one-dimensional chain complexes of general formula $KLn(OAr)_4$ (Ln = La, Nd, Sm, Er) are quite diverse and will be the subject of a separate publication.[19,33b]

$$LnCl_3 + 3KOAr \xrightarrow{THF} Ln(OAr)_3(THF)_2 + 3KCl \quad (6)$$

Ln = Sm (**5**), Pr (**8**), Gd (**9**), Yb (**10**); Ar = $2,6\text{-}i\text{-}Pr_2C_6H_3$

$$LnCl_3 + 4KOAr \xrightarrow{THF} KLn(OAr)_4 + 3KCl \quad (7)$$

Ln = Nd, Er; Ar = $2,6\text{-}i\text{-}Pr_2C_6H_3$

Solid State and Molecular Structures. Six lanthanide complexes containing 2,6-diisopropylphenoxide ligation have been examined by single-crystal X-ray diffraction techniques during the course of this work: $Ln_2(OAr)_6$ (Ln = Nd (**1**), Sm (**2**); Ar = $2,6\text{-}i\text{-}Pr_2C_6H_3$) and $Ln(OAr)_3(THF)_2$ (Ln = Er (**6**), Lu (**7**), Pr (**8**), Gd (**9**); Ar = $2,6\text{-}i\text{-}Pr_2C_6H_3$). Data collection parameters are given in Table 1, selected fractional coordinates are given in Tables 2–7, selected bond lengths and angles for **1** and **2** are listed in Table 8, and selected bond lengths and angles for **6**–**9** are given in Table 9.

$Ln_2(OAr)_6$ Complexes. Single crystals of **1** (Ln = Nd) and **2** (Ln = Sm) were grown from concentrated toluene solutions at −40 °C, and their structures were determined from diffraction data collected at −162 and −70 °C, respectively. In the solid state, both **1** and **2** revealed centrosymmetric, dimeric $Ln_2(O\text{-}2,6\text{-}i\text{-}Pr_2C_6H_3)_6$ units bridged by intermolecular η^6-π-arene interactions of a unique aryloxide ligand as shown in Figure 1. The coordination geometry of each lanthanide atom approximates a three-legged piano stool. Each metal is bound to three terminal aryloxide oxygen atoms, and six carbon atoms of one of the aromatic rings of an aryloxide ligand are bound to the symmetry-related metal atom in the dimeric unit (Figure 1). The overall structure is thus identical to that previously described for the uranium(III) aryloxide complex $U_2(O\text{-}2,6\text{-}i\text{-}Pr_2C_6H_3)_6$ (**11**),[32] with the neodymium complex **1** being isostructural with its uranium analog. The lanthanide–oxygen bond lengths average 2.122(9) (Ln = Nd, **1**) and 2.101(6) Å (Sm, **2**) for terminal ligands and 2.211(9) (Nd, **1**) and 2.198(5) Å (Sm, **2**) for bridging aryloxide ligands. The Ln–O–C bond angles average 161.8(5) and 163.0(9)° for **1** and **2**, respectively. The average terminal Nd–O distance of 2.122(9) Å can be compared to average terminal

Table 2. Selected Fractional Coordinates and Isotropic Thermal Parameters[a] for the $Nd_2(O\text{-}2,6\text{-}i\text{-}Pr_2C_6H_3)_6$ Molecule (**1**)

	10^4x	10^4y	10^4z	$10B_{iso}$, Å²
Nd(1)	709(1)	95.6(3)	6666.7(5)	22
O(2)	1683(7)	5(4)	5630(5)	32
C(3)	1864(10)	−138(6)	4922(7)	28
C(4)	2332(12)	304(5)	4435(7)	17
C(5)	2492(11)	129(6)	3681(8)	25
C(6)	2231(13)	−483(7)	3394(9)	33
C(7)	1767(13)	−928(6)	3909(11)	37
C(8)	1577(13)	−775(6)	4627(12)	40
C(9)	2861(12)	936(5)	4797(8)	25
C(12)	1126(19)	−1258(7)	5173(14)	68
O(15)	1573(10)	884(4)	7390(6)	40
C(16)	2015(14)	1289(6)	8009(9)	24
C(17)	3145(13)	1716(5)	7969(8)	23
C(18)	3582(12)	2139(5)	8612(9)	26
C(19)	2964(14)	2155(7)	9249(10)	35
C(20)	1877(13)	1719(7)	9274(9)	35
C(21)	1400(13)	1290(7)	8652(9)	32
C(22)	3856(13)	1709(5)	7273(9)	28
C(25)	221(17)	802(8)	8711(9)	49
O(28)	1492(8)	−686(4)	7420(5)	22
C(29)	2208(13)	−1055(6)	8039(9)	26
C(30)	1497(13)	−1605(6)	8199(8)	26
C(31)	2213(15)	−1975(7)	8848(9)	35
C(32)	3540(17)	−1812(8)	9321(9)	43
C(33)	4236(13)	−1273(8)	9132(9)	40
C(34)	3591(13)	−904(6)	8500(8)	30
C(35)	25(14)	−1757(6)	7706(9)	32
C(38)	4352(15)	−325(7)	8262(10)	39

[a] Isotropic values for those atoms refined anisotropically are calculated by using the formula given by: Hamilton, W. C. *Acta Crystallogr.* **1959**, *12*, 609.

Nd–O distances of 2.153(4), 2.146(4), 2.145(6), 2.05(2), 2.174(2), 2.148(16), 2.138(8), and 2.162(5) Å seen in the aliphatic alkoxide complexes $Nd_2(OCH\text{-}i\text{-}Pr_2)_6(THF)_2$,[33a] $Nd_2(OCH\text{-}i\text{-}Pr_2)_6(py)_2$,[33a] $Nd_2(OCH\text{-}i\text{-}Pr_2)_6(\mu\text{-dme})$,[33a] $Nd_6(O\text{-}i\text{-}Pr)_{17}Cl$,[34] $Nd(OC\text{-}t\text{-}Bu_2CH_2PMe_2)_3$,[35] $Nd_5O(O\text{-}i\text{-}Pr)_{13}(HO\text{-}i\text{-}Pr)_2$,[36] $Nd_4(OCH_2\text{-}t\text{-}Bu)_{12}$,[37] and $Nd(OC\text{-}t\text{-}Bu_3)_3(CH_3CN)_2$,[23] respectively.

(34) Andersen, R. A.; Templeton, D. H. Zalkin, A. *Inorg. Chem.* **1978**, *17*, 1962.
(35) Hitchcock, P. B.; Lappert, M. F.; MacKinnon, I. A. *J. Chem. Soc., Chem. Commun.* **1988**, 1557.
(36) Helgesson, G.; Jagner, S.; Poncelet, O.; Hubert-Pfalzgraf, L. G. *Polyhedron* **1991**, *10*, 1559.
(37) Barnhart, D. M.; Clark, D. L.; Gordon, J. C.; Huffman, J. C.; Watkin, J. G.; Zwick, B. D. *J. Am. Chem. Soc.* **1993**, *115*, 8461.

Table 3. Selected Atomic Coordinates and Equivalent Isotropic Displacement Coefficients[a] for One of the Molecules in the Asymmetric Unit of the $Sm_2(O\text{-}2,6\text{-}i\text{-}Pr_2C_6H_3)_6$ Molecule (**2**)

	10^4x	10^4y	10^4z	$10^3U(eq)$, Å^2
Sm(1)	210(1)	175(1)	820(1)	20(1)
O(2)	−1356(6)	95(2)	328(2)	26(2)
C(3)	−1898(8)	−113(4)	−16(2)	22(3)
C(4)	−1782(8)	−760(3)	−114(2)	20(3)
C(5)	−2355(8)	−977(4)	−477(3)	30(3)
C(6)	−3020(8)	−558(4)	−745(2)	29(3)
C(7)	−3176(8)	65(4)	−643(2)	27(3)
C(8)	−2641(8)	304(4)	−278(2)	26(3)
C(9)	−1123(9)	−1204(4)	200(3)	33(3)
C(12)	−2944(9)	948(4)	−125(3)	30(3)
O(15)	−193(6)	964(3)	1178(2)	30(2)
C(16)	−652(10)	−930(4)	1528(2)	31(3)
C(17)	88(10)	−1476(5)	1625(3)	44(4)
C(18)	−366(13)	−1829(5)	1955(3)	63(5)
C(19)	−1498(12)	−1628(5)	2176(3)	58(4)
C(20)	−2202(10)	−1095(5)	2078(3)	46(4)
C(21)	−1796(9)	−729(4)	1742(3)	33(3)
C(22)	1324(12)	−1674(5)	1391(4)	61(4)
C(25)	−2673(10)	−166(5)	1623(3)	49(4)
O(28)	−202(6)	−574(3)	1210(2)	29(2)
C(29)	−400(8)	1344(4)	1494(3)	26(3)
C(30)	548(8)	1332(4)	1822(3)	29(3)
C(31)	351(9)	1742(5)	2145(3)	40(3)
C(32)	−778(10)	2157(5)	2140(3)	44(4)
C(33)	−1698(9)	2157(4)	1816(3)	35(3)
C(34)	−1552(8)	1748(4)	1489(2)	27(3)
C(35)	1738(9)	852(4)	1842(3)	38(3)
C(38)	−2544(9)	1757(4)	1131(3)	35(3)

[a] Equivalent isotropic U defined as one-third of the trace of the orthogonalized $\mathbf{U}_{ij}$ tensor.

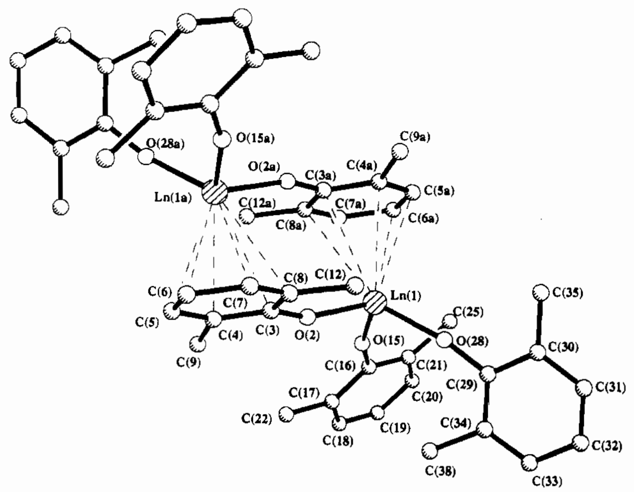

Figure 1. Ball-and-stick drawing emphasizing the centrosymmetric π-arene-bridged dimeric structure of $Ln_2(OAr)_6$ complexes (Ln = Nd (**1**), Sm (**2**); Ar = $2,6\text{-}i\text{-}Pr_2C_6H_3$) and giving the atom-numbering scheme used in the tables.

In a similar fashion, the average terminal Sm–O distance of 2.101(6) Å can be compared to the Sm–O distance of 2.13(1) Å found in the aryloxide ligand of $(\eta\text{-}C_5Me_5)_2Sm(O\text{-}2,3,5,6\text{-}Me_4C_6H)$[38] and the average Sm–O distances of 2.08(2) and 2.099(9) Å found for the alkoxide ligands in $[(\eta\text{-}C_5Me_5)_2Sm]_2(O_2C_{16}H_{10})$[39] and $[(\eta\text{-}C_5Me_5)_2Sm(THF)]_2(O_2C_{16}H_{10})$,[39] respectively.

Two η^6-arene bridges hold the dimeric units together with an average Ln–C distance of 3.035 Å for **1** (Nd–C range 2.898(12)–3.183(10) Å) and 2.986 and 3.016 Å for the two independent molecules in the asymmetric unit of **2** (Sm–C ranges 2.847(8)–3.135(8) Å and 2.824(7)–3.160(8) Å, respectively). These average Ln–C bond distances are in the same range as those observed in the other known examples of trivalent 4f element–π-arene interactions and can be compared with 2.89(3), 2.91(6), 2.93(3), 2.90(4) 2.999(23), and 2.978(6) Å observed for the average Ln–C distances found in $(\eta\text{-}C_6Me_6)Sm(AlCl_4)_3$,[40] $(\eta\text{-}C_6H_6)Sm(AlCl_4)_3$,[41] $(\eta\text{-}C_6H_6)Nd(AlCl_4)_3$,[41] $(\eta\text{-}1,3\text{-}Me_2C_6H_4)Sm(AlCl_4)_3$,[42] $[(\eta\text{-}C_6Me_6)Eu(AlCl_4)_3]_4$,[43] and $Yb(O\text{-}2,6\text{-}Ph_2C_6H_3)_3$.[25] These distances are, however, significantly longer than the Gd–C distance of 2.630(4) Å found for the zerovalent $Gd(\eta\text{-}t\text{-}Bu_3C_6H_3)_2$.[44] The nonbonding metal–metal distances within the dimers are 5.53 and 5.11 Å for **1** and **2**, respectively.

Examples of η^6-coordination of an arene ring to a lanthanide metal center are relatively rare, and the only examples that we are aware of are those listed above. The known 4f element–π-arene complexes display three basic structural types for $[(\eta\text{-arene})Ln(AlCl_4)_3]_x$, $Yb(O\text{-}2,6\text{-}Ph_2C_6H_3)_3$, and $(\eta\text{-arene})_2Gd$ which are illustrated qualitatively in **I–III**. An interesting comparison may

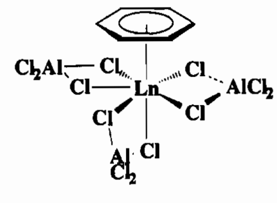

I

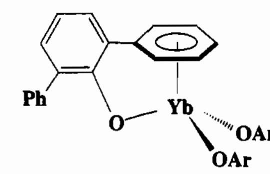

II

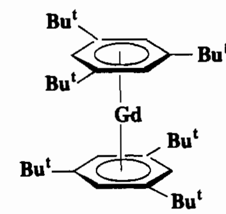

III

be drawn between the π-arene dimers, **1** (Nd) and **2** (Sm), and the ytterbium complex shown schematically in **II**. The lanthanide coordination environments are essentially identical in each case, but in **II** the π-arene interaction required to complete the coordination sphere is accomplished by means of an *intra*molecular contact with a phenyl ring in the 2- or 6-position of the aryloxide ligand. Finally, while the π-arene-bridged dimeric unit observed in the solid state for **1** and **2** has been observed in 5f element chemistry;[32] it constitutes a new structural type for 4f element–π-arene complexes as illustrated in **IV**.

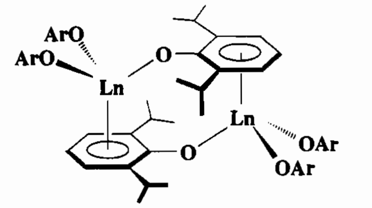

IV

$Ln(OAr)_3(THF)_2$ Complexes. The four THF bisadducts subjected to X-ray diffraction analysis $Ln(O\text{-}2,6\text{-}i\text{-}Pr_2C_6H_3)_3(THF)_2$ (Ln = Er (**6**), Lu(**7**), Pr (**8**), Gd (**9**)) are isostructural; hence their solid state structures are discussed concurrently. Crystals of compounds **6-9** were grown by slow evaporation of

(38) Evans, W. J.; Hanusa, T. P.; Levan, K. R. *Inorg. Chim. Acta* **1985**, *110*, 191.
(39) Evans, W. J.; Drummond, D. K.; Hughes, L. A.; Zhang, H.; Atwood, J. L. *Polyhedron* **1988**, *7*, 1693.
(40) Cotton, F. A.; Schwotzer, W. *J. Am. Chem. Soc.* **1986**, *108*, 4657.
(41) Fan, B.; Shen, Q.; Lin, Y. *J. Organomet. Chem.* **1989**, *377*, 51.
(42) Fan, B.; Shen, Q.; Lin, Y. *J. Organomet. Chem.* **1989**, *376* 61.
(43) Liang, H.; Shen, Q.; Jin, S.; Lin, Y, *J. Chem. Soc., Chem. Commun.* **1992**, *6*, 480.
(44) Brennan, J. G.; Cloke, F. G. N.; Sameh, A. A.; Zalkin, A. *J. Chem. Soc., Chem. Commun.* **1987**, 1668.

Table 4. Selected Fractional Coordinates and Isotropic Thermal Parameters[a] for the $Er(O\text{-}2,6\text{-}i\text{-}Pr_2C_6H_3)_3(THF)_2$ Molecule (**6**)

	10^4x	10^4y	10^4z	$10B_{iso}$, Å^2
Er(1)	2147(1)	1196	2872.9(4)	9
O(1)	1438(11)	1592(6)	1163(9)	12(2)
O(2)	1544(10)	1799(5)	4061(8)	8(2)
O(3)	3306(10)	275(5)	2967(8)	9(2)
O(4)	4430(11)	1747(6)	3666(9)	12(2)
O(5)	162(11)	483(6)	2824(9)	13(2)
C(1)	609(15)	2043(8)	342(12)	8(2)
C(2)	−801(16)	1837(8)	−329(14)	10(3)
C(3)	−1707(19)	2298(10)	−1147(15)	21(3)
C(4)	−1147(20)	2997(10)	−1220(16)	25(3)
C(5)	287(18)	3149(9)	−557(15)	17(3)
C(6)	1135(17)	2697(9)	223(13)	13(3)
C(7)	−1402(14)	1085(8)	−161(11)	10(3)
C(10)	2727(19)	2857(9)	898(14)	17(3)
C(13)	968(17)	2187(9)	4768(14)	15(3)
C(14)	303(17)	2833(9)	4341(13)	14(3)
C(15)	−239(16)	3214(8)	5000(14)	12(3)
C(16)	−180(19)	2977(10)	6114(15)	20(3)
C(17)	532(16)	2341(8)	6561(13)	13(3)
C(18)	1118(16)	1966(8)	5879(13)	13(3)
C(19)	131(23)	3046(11)	3093(18)	30(4)
C(22)	1886(14)	1158(12)	6335(11)	13(2)
C(25)	4171(15)	−298(8)	3087(12)	6(2)
C(26)	4993(15)	−505(8)	4249(12)	8(2)
C(27)	5899(17)	−1099(9)	4332(13)	13(3)
C(28)	6028(18)	−1440(9)	3398(14)	17(3)
C(29)	5210(18)	−1224(9)	2322(15)	19(3)
C(30)	4279(14)	−649(7)	2123(11)	7(2)
C(31)	4884(17)	−120(8)	5317(13)	13(3)
C(34)	3430(17)	−336(8)	889(13)	10(3)
C(37)	4721(21)	2371(11)	4404(17)	26(4)
C(38)	6216(40)	2249(21)	5214(32)	75(8)
C(39)	6985(26)	1802(14)	4697(21)	42(5)
C(40)	5834(18)	1486(9)	3660(14)	19(3)
C(41)	−1073(21)	635(11)	3208(17)	26(4)
C(42)	−1698(16)	−56(8)	3329(13)	10(3)
C(43)	−1572(18)	−434(8)	2276(13)	10(3)
C(44)	−47(19)	−207(10)	2283(16)	21(3)

[a] Isotropic values for those atoms refined anisotropically are calculated by using the formula given by: Hamilton, W. C. *Acta Crystallogr.* **1959**, *12*, 609.

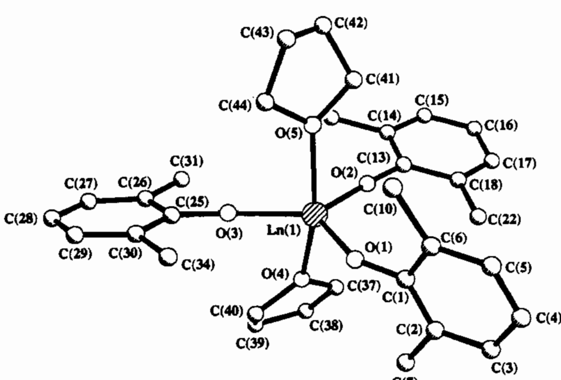

Figure 2. Ball-and-stick drawing emphasizing the trigonal bipyramidal coordination geometry of $Ln(OAr)_3(THF)_2$ complexes (Ln = Er (**6**), Lu (**7**), Pr (**8**), Gd (**9**); Ar = 2,6-i-$Pr_2C_6H_3$) and giving the atom-numbering scheme used in the tables.

toluene solutions in the drybox atmosphere. Data were collected at −170 °C (**6**) or at −70 °C (**7**–**9**). The compounds all crystallize in the monoclinic space group $P2_1$ as discrete molecules with no unusual intermolecular contacts. The overall molecular structure in the solid state consists of a lanthanide metal center coordinated in a distorted trigonal bipyramidal fashion by three equatorial aryloxide and two axial THF ligands as shown in Figure 2. Trigonal bipyramidal coordination has been observed previously in structurally characterized $Ln(OR)_3(L)_2$ complexes such as $Nd(OC\text{-}t\text{-}Bu_3)_3(CH_3CN)_2$[23] and $Ce(O\text{-}2,6\text{-}t\text{-}Bu_2C_6H_3)_3(CN\text{-}t\text{-}Bu)_2$,[13a] although the latter complex features one axial and one

Table 5. Selected Atomic Coordinates and Equivalent Isotropic Displacement Coefficients[a] for the $Lu(O\text{-}2,6\text{-}i\text{-}Pr_2C_6H_3)_3(THF)_2$ Molecule (**7**)

	10^4x	10^4y	10^4z	10^3U(eq), Å^2
Lu(1)	2104(1)	1295	7866(1)	19(1)
O(1)	1423(3)	892(2)	6219(3)	28(1)
O(2)	1475(3)	728(2)	9043(3)	28(1)
O(3)	3250(3)	2197(2)	7958(3)	27(1)
O(4)	4336(4)	753(2)	8675(3)	31(1)
O(5)	154(4)	2003(2)	7787(3)	28(1)
C(1)	646(6)	443(3)	5397(4)	29(2)
C(2)	−785(7)	630(4)	4684(5)	34(2)
C(3)	−1631(6)	139(5)	3871(5)	53(3)
C(4)	−1045(8)	−492(5)	3772(5)	56(3)
C(5)	396(8)	−660(4)	4456(5)	47(2)
C(6)	1245(6)	−197(3)	5246(4)	35(2)
C(7)	−1383(5)	1368(7)	4824(4)	43(2)
C(10)	2839(7)	−361(4)	5971(5)	39(2)
C(13)	957(5)	330(3)	9724(4)	22(1)
C(14)	271(5)	−311(3)	9282(4)	28(2)
C(15)	−254(6)	−717(3)	9994(5)	38(2)
C(16)	−156(6)	−504(3)	11099(5)	37(2)
C(17)	521(5)	113(3)	11528(4)	35(2)
C(18)	1103(5)	541(3)	10864(4)	25(2)
C(19)	91(6)	−526(3)	8048(5)	37(2)
C(22)	1849(5)	1228(6)	11331(4)	38(2)
C(25)	4119(5)	2751(3)	8086(4)	23(1)
C(26)	4942(5)	2994(3)	9224(4)	26(2)
C(27)	5850(5)	3565(3)	9342(5)	36(2)
C(28)	5940(6)	3920(3)	8385(5)	39(2)
C(29)	5126(6)	3686(3)	7275(5)	35(2)
C(30)	4220(5)	3111(3)	7102(4)	28(2)
C(31)	4778(6)	2613(3)	10284(5)	35(2)
C(34)	3387(7)	2813(4)	5912(5)	33(2)
C(37)	4609(6)	132(4)	9402(7)	53(3)
C(38)	6136(8)	129(7)	10081(10)	125(6)
C(39)	6878(7)	681(5)	9696(8)	75(3)
C(40)	5758(5)	988(4)	8640(5)	40(2)
C(41)	−1101(6)	1842(3)	8164(5)	38(2)
C(42)	−1734(6)	2524(3)	8287(5)	39(2)
C(43)	−1541(8)	2937(4)	7280(7)	36(2)
C(44)	3(6)	2711(3)	7330(6)	37(2)

[a] Equivalent isotropic U defined as one-third of the trace of the orthogonalized U_{ij} tensor.

equatorial isocyanide ligand. Ln–O distances for the aryloxide ligands average 2.078 (**6**, Nd), 2.044 (**7**, Lu), 2.172 (**8**, Pr), and 2.130 Å (**9**, Gd), which are among the shortest Ln–O distances yet observed for molecular complexes containing these four lanthanide metals. This may reflect the fact that these are among the first alkoxide or aryloxide structures of praseodymium, gadolinium, erbium, and lutetium to be reported. A short terminal Gd–O distance of 2.08(2) Å is seen in $Na_2[Gd_4(O\text{-}t\text{-}Bu)_4(\mu_3\text{-}O\text{-}t\text{-}Bu)_8(\mu_6\text{-}O)]$,[9] which is the only other alkoxide or aryloxide structure of these four metals of which we are aware. The vast majority of Ln–O interactions reported to date for these metals have been with bidentate ligands such as acetate and oxalate, multidentate Schiff base ligands, or ligands with ether type linkages. For example, in the complex $K_3[Gd(C_2O_4)_3(H_2O)]\text{-}(H_2O)_2$,[45] Gd–O distances average 2.447(2) Å, compared to the 2.130 Å average distance in **9**, while Pr–O distances average 2.427(5) Å in $[Pr_2(H_2O)_{11}(C_4O_4)_3](H_2O)_2$[46] and 2.45(2) Å in $[NBu_4][Pr(C_8H_4F_3O_2S)_4]$,[47] compared to 2.172 Å in **8**. Somewhat shorter Ln–O distances can be found in the aryloxide linkages of $Pr(C_{17}H_{29}N_4O_3)(NO_3)_2(CH_3OH)$ [Pr–O = 2.263(3) Å][48] and $Er(salen)_2(pipH)$ [Er–O = 2.22(1) Å][49] (salen = ethylenebis-(salicylaldimine), pipH = piperidine), but these distances are

(45) Kahwa, I. A.; Fronczek, F. R.; Selbin, J. *Inorg. Chim. Acta* **1984**, *82*, 161.
(46) Petit, J.-F.; Gleizes, A.; Trombe, J.-C. *Inorg. Chim. Acta* **1990**, *167*, 51.
(47) Criasia, R. T. *Inorg. Chim. Acta* **1987**, *133*, 189.
(48) Kahwa, I. A.; Fronczek, F. R.; Selbin, J. *Inorg. Chim. Acta* **1987**, *126*, 227.
(49) Mangani, S.; Takeuchi, A.; Yamada, S.; Orioli, P. *Inorg. Chim. Acta* **1989**, *155*, 149.

Table 6. Selected Atomic Coordinates and Equivalent Isotropic Displacement Coefficients[a] for the $Pr(O\text{-}2,6\text{-}i\text{-}Pr_2C_6H_3)_3(THF)_2$ Molecule (**8**)

	10^5x	10^5y	10^5z	10^4U(eq), Å^2
Pr(1)	22235(5)	0	78882(4)	229(2)
O(1)	14173(89)	−4015(46)	61350(70)	345(31)
O(2)	15688(86)	−5986(42)	91262(66)	309(29)
O(3)	33767(85)	9878(45)	79572(79)	369(32)
O(4)	46063(88)	−5459(45)	87295(77)	377(32)
O(5)	1731(93)	7625(44)	78822(77)	374(33)
C(1)	5712(124)	−8507(67)	53264(90)	287(41)
C(2)	−8719(148)	−6687(100)	46497(122)	433(59)
C(3)	−16894(167)	−11486(103)	38994(123)	582(68)
C(4)	−11369(202)	−18133(121)	38075(138)	734(81)
C(5)	2278(170)	−19688(83)	44365(127)	511(61)
C(6)	11434(136)	−15075(70)	52067(105)	355(47)
C(7)	−13920(139)	524(175)	47938(108)	608(58)
C(10)	26930(184)	−16565(82)	59049(138)	473(62)
C(13)	10260(123)	−9616(64)	98204(101)	292(41)
C(14)	3158(119)	−16033(62)	93994(102)	282(40)
C(15)	−2064(137)	−19788(72)	101477(127)	405(50)
C(16)	−951(147)	−17403(74)	112250(116)	416(52)
C(17)	6165(138)	−11233(65)	116497(103)	345(44)
C(18)	11554(118)	−7186(60)	109494(95)	263(39)
C(19)	1668(135)	−18363(74)	81833(113)	378(48)
C(22)	19256(130)	−549(124)	113942(100)	403(45)
C(25)	42381(122)	15509(62)	80824(106)	303(41)
C(26)	50190(131)	18012(74)	91957(122)	384(49)
C(27)	58954(166)	23578(78)	92630(137)	481(57)
C(28)	59756(142)	26802(70)	82755(155)	517(63)
C(29)	51632(141)	24401(66)	71843(126)	395(51)
C(30)	42842(120)	18550(58)	70390(109)	283(42)
C(31)	48769(174)	14133(99)	102474(145)	595(70)
C(34)	34386(160)	15449(79)	58468(124)	378(55)
C(37)	49041(185)	−11479(103)	94735(169)	701(80)
C(38)	63122(199)	−10412(158)	103357(209)	1251(131)
C(39)	70214(188)	−5337(121)	98535(217)	972(99)
C(40)	59748(115)	−2839(79)	87547(129)	460(52)
C(41)	−10445(155)	5939(82)	82381(154)	558(66)
C(42)	−17572(167)	12629(81)	82925(142)	521(62)
C(43)	−15206(207)	16670(84)	72793(170)	391(58)
C(44)	−305(163)	14526(75)	73936(154)	496(65)

[a] Equivalent isotropic U defined as one-third of the trace of the orthogonalized U_{ij} tensor.

Table 7. Selected Atomic Coordinates and Equivalent Isotropic Displacement Coefficients[a] for the $Gd(O\text{-}2,6\text{-}i\text{-}Pr_2C_6H_3)_3(THF)_2$ Molecule (**9**)

	10^4x	10^4y	10^4z	10^3U(eq), Å^2
Gd(1)	2140(1)	0	7857(1)	22(1)
O(1)	1404(11)	445(5)	6151(8)	37(2)
O(2)	1531(11)	606(5)	9105(8)	39(2)
O(3)	3335(8)	−913(5)	7982(7)	26(2)
O(4)	4463(10)	596(6)	8680(10)	44(2)
O(5)	127(10)	−686(5)	7787(8)	37(2)
C(1)	590(14)	901(8)	5336(11)	33(2)
C(2)	−830(15)	705(10)	4651(12)	45(2)
C(3)	−1651(17)	1222(11)	3886(13)	59(2)
C(4)	−1180(17)	1855(12)	3729(13)	68(2)
C(5)	316(18)	2004(9)	4420(13)	54(2)
C(6)	1175(15)	1545(8)	5211(11)	38(2)
C(7)	−1424(12)	−36(15)	4789(10)	53(2)
C(10)	2796(17)	1666(9)	5947(13)	45(2)
C(13)	988(12)	1019(7)	9782(10)	26(2)
C(14)	314(13)	1642(8)	9348(12)	34(2)
C(15)	−235(14)	2024(8)	10057(13)	38(2)
C(16)	−122(14)	1814(8)	11153(12)	41(2)
C(17)	558(14)	1187(8)	11589(11)	36(2)
C(18)	1103(14)	783(8)	10903(11)	32(2)
C(19)	110(15)	1872(8)	8122(11)	37(2)
C(22)	1882(12)	67(13)	11360(10)	44(2)
C(25)	4166(14)	−1478(7)	8128(11)	30(2)
C(26)	4951(14)	−1697(8)	9200(12)	35(2)
C(27)	5866(14)	−2270(7)	9310(13)	36(2)
C(28)	5967(15)	−2619(8)	8331(14)	45(2)
C(29)	5146(15)	−2380(8)	7229(14)	41(2)
C(30)	4267(13)	−1800(6)	7099(12)	30(2)
C(31)	4799(15)	−1334(9)	10254(12)	43(2)
C(34)	3404(16)	−1493(9)	5864(13)	44(2)
C(37)	4711(17)	1209(10)	9402(18)	67(2)
C(38)	6158(18)	1166(15)	10213(20)	113(2)
C(39)	6938(18)	606(12)	9800(19)	91(2)
C(40)	5834(14)	354(9)	8680(17)	62(2)
C(41)	−1149(14)	−511(8)	8154(14)	39(2)
C(42)	−1767(14)	−1218(8)	8279(13)	39(2)
C(43)	−1540(14)	−1625(7)	7277(11)	29(2)
C(44)	−73(15)	−1382(8)	7309(12)	37(2)

[a] Equivalent isotropic U defined as one-third of the trace of the orthogonalized U_{ij} tensor.

still *ca.* 0.1 Å longer than those observed in the aryloxide complexes **6** (Er) and **8** (Pr).

Lanthanide–oxygen distances for the THF ligands average 2.346(2) (**6**, Er), 2.296(2) (**7**, Lu), 2.482(8) (**8**, Pr), and 2.394(15) Å (**9**, Gd). The average Pr–O distance of 2.482(8) Å seen in **8** is somewhat shorter than those observed in $Cp_3Pr(THF)$ (2.56(1) Å),[50] $(\eta\text{-}C_8H_8)Pr(\eta\text{-}C_5H_5)(THF)_2$ (2.610 Å average)[51] or $(\eta\text{-}C_8H_8)Pr(\eta^5\text{-}C_9H_7)(THF)_2$ (2.638 Å average),[51] while the Lu–O distance of 2.296(2) Å in **7** lies between that observed in $Cp_3Lu(THF)$ (2.39(2) Å)[52] and those found for $Cp_2Lu(CH_2SiMe_3)(THF)$ (2.228(10) Å)[53] and $Cp_2Lu(4\text{-}MeC_6H_4)(THF)$ (2.265(28) Å).[53] The average Er–O distance of 2.346(2) Å in **6** is similar to the distances seen in $CpErCl_2(THF)_3$ (2.350(3), 2.365(3), and 2.452(3) Å),[54] while the average Gd–O distance of 2.394(15) Å in **9** is shorter than those observed in $Cp_3Gd(THF)$ (2.494(7) Å)[55] and $\{Gd[N(SiMe_3)_2]_2Cl(THF)\}_2$ (2.444(5) Å).[56]

(50) Yuguo, F.; Pinzhe, L.; Zhongsheng, J.; Wenqi, C. *Sci. Scin., Ser. B* **1984**, *27*, 993.
(51) Ke, W.; Zhongsheng, J.; Wenqi, C. *J. Chem. Soc., Chem. Commun.* **1991**, 680.
(52) Ni, C.; Deng, D.; Qian, C. *Inorg. Chim. Acta* **1985**, *110*, L7.
(53) Schumann, H.; Genthe, W.; Bruncks, N.; Pickardt, J. *Organometallics* **1982**, *1*, 1194.
(54) Day, C. S.; Day, V. W.; Ernst, R. D.; Vollmer, S. H. *Organometallics* **1982**, *1*, 998.
(55) Rogers, R. D.; Vann Bynum, R.; Atwood, J. L. *J. Organomet. Chem.* **1980**, *192*, 65.
(56) Aspinall, H. C.; Bradley, D. C.; Hursthouse, M. B.; Sales, K. D.; Walker, N. P. C.; Hussain, B. *J. Chem. Soc., Dalton Trans.* **1989**, 623.

A common feature seen in all $Ln(OAr)_3(THF)_2$ structures is that two of the aryloxide ligands lie with their phenyl rings almost in the equatorial plane of the trigonal bipyramid, whereas the third aryloxide ligand [containing O(1)] is twisted noticeably out of this plane, presumably owing to the steric bulk of the diisopropylphenoxide ligands (Figure 2). The Ln–O–C angle of this unique aryloxide ligand (150.7(9), 153.0(4), 150.9(8), and 152.8(10)° for **6** (Er), **7** (Lu), **8** (Pr), and **9** (Gd)) is in all cases about 20° smaller than the average Ln–O–C angle for the other two aryloxide ligands (174.0, 174.3, 173.5, and 174.4° for **6**–**9** respectively). The axial THF ligands bend away from this unique aryloxide ligand, resulting in an axial O–Ln–O angle between THF ligands that is significantly smaller than 180° in all of the structures, measuring 157.8(4), 157.5(1), 155.9(3), and 158.9(4)° for **6** (Er), **7** (Lu), **8** (Pr), and **9** (Gd), respectively.

Spectroscopic Characterization

NMR Studies. $Ln_2(OAr)_6$ Complexes. Ambient temperature ^1H and ^{13}C NMR spectra of the $Ln_2(OAr)_6$ complexes **1** and **2** in benzene-d_6 and in toluene-d_8 solution clearly show the presence of *two* aryloxide environments in a 2:1 ratio, suggesting that a dimeric structure is *retained* in solution. Complete spectral assignment of all ^{13}C resonances in the neodymium complex (**1**) is precluded by the fact that the paramagnetism of this species causes the aryloxide ring carbon resonances to be obscured by those of the aromatic solvent. Oxygen- or halogen-containing solvents were found to react with these molecules, and they are too insoluble in methylcyclohexane-d_{14} to obtain a ^{13}C NMR

Table 8. Selected Bond Distances (Å) and Angles (deg) for $Ln_2(O\text{-}2,6\text{-}i\text{-}Pr_2C_6H_3)_6$ Molecules

	Ln			Ln	
	Nd (1)	Sm (2)		Nd (1)	Sm (2)
Ln(1)–O(2)	2.211(8)	2.195(5)	Ln(1)–O(15)	2.124(9)	2.099(6)
Ln(1)–O(28)	2.120(8)	2.097(5)	Ln(1)–C(3A)	3.183(10)	3.160(8)
Ln(1)–C(4A)	3.157(11)	3.084(8)	Ln(1)–C(5A)	2.998(10)	2.922(8)
Ln(1)–C(6A)	2.898(12)	2.824(7)	Ln(1)–C(7A)	2.917(12)	2.955(8)
Ln(1)–C(8A)	3.058(15)	3.148(8)	O(2)–C(3)	1.305(15)	1.318(9)
O(15)–C(16)	1.349(17)	1.345(10)	O(28)–C(29)	1.359(15)	1.378(10)

	Ln	
	Nd (1)	Sm (2)
O(2)–Ln(1)–O(15)	111.0(4)	110.6(2)
O(2)–Ln(1)–O(28)	105.6(3)	105.5(2)
O(15)–Ln(1)–O(28)	103.5(3)	102.6(2)
Ln(1)–O(2)–C(3)	161.6(7)	156.5(5)
Ln(1)–O(15)–C(16)	163.9(9)	163.1(5)
Ln(1)–O(28)–C(29)	163.6(8)	163.6(5)

spectrum. It is clear, however, that, as for the samarium analog, there are two distinct aryloxide environments in the neodymium complex (**1**) since two types of isopropyl groups (^1H and ^{13}C), as well as two distinct types of *ipso* ring carbon resonances (^{13}C), are observed in a 2:1 ratio. While these NMR spectral data alone cannot distinguish between a π-arene-bridged structure (**IV**) and the oxygen-bridged structure **V**, a careful consideration of chemical shift values and the degree of line broadening provides more insight into the solution structure.

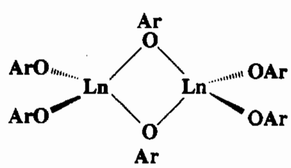

V

^1H NMR spectra reveal that the Sm(III) metal center in **2** exhibits a relatively small paramagnetic influence upon the chemical shift range compared to the neodymium(III) center in **1**. In the ^1H NMR spectra of both molecules, the resonances assigned to the methine isopropyl proton of the bridging aryloxide ligand are shifted noticeably downfield compared to the position of the methine proton resonance of the terminal aryloxides. This effect is magnified in the neodymium complex (**1**) [δ 40.62 (bridging) *vs* 8.18 (terminal)] compared to the samarium analog (**2**) [δ 11.81 (bridging) *vs* 4.21 (terminal)]. These data suggest that bridging and terminal aryloxide ligands occupy very dissimilar environments in solution. Additionally, the *meta* and *para* proton resonances of the bridging ligand are shifted considerably *upfield* relative to the terminal ligands, with the effect again being greater in the neodymium compound **1** [δ −20.25 (*meta*, bridge) and −44.41 (*para*, bridge) vs 13.23 (*meta*, terminal) and 10.28 (*para*, terminal)]. The large shift difference between the aromatic protons of bridging and terminal ligands further suggests that the arene ring of the bridging ligand experiences an environment significantly different from those of the terminal ligands and could be consistent with structure **IV**.

Comparison of $^{13}C\{^1H\}$ NMR spectra for **1** and **2** reveals that resonances assigned to aryloxide *ipso* carbons (*i.e.* those bound directly to the oxygen atoms) in Nd complex **1** (δ 219.0 and 225.1) are shifted *noticeably* downfield and significantly broadened relative to the corresponding resonances for the Sm analog (δ 162.3 and 164.8). The increased line broadening of the less intense, higher field resonance at δ 219.0 in **1** could be consistent with the proposal that one 2,6-diisopropylphenoxide ligand is bound directly to a lanthanide center in an η^6-fashion (structure type **IV**) rather than indirectly through a μ_2-oxygen bridged mode (structure type **V**) or in a monomeric $Ln(OAr)_3$ complex. If the latter structure were present in solution, the *ipso* carbon atoms of the aryloxide ligand would not be involved in direct binding interaction with a metal center, and thus **1** would not be expected to show the substantial difference in line broadening between *ipso* carbons of the terminal and bridging ligands. While these NMR data alone are not conclusive evidence for structure type **IV**, additional compelling evidence is obtained from solid state and solution infrared spectra.

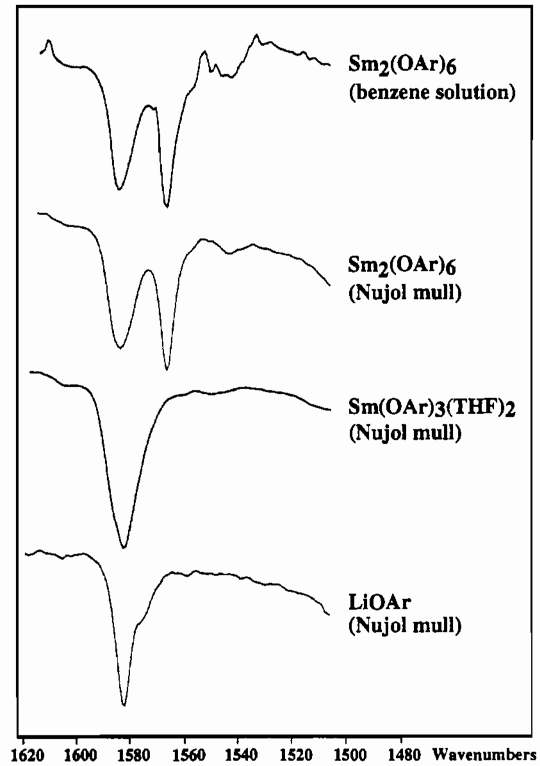

Figure 3. Comparison of the crucial ν(C=C) stretching regions of the IR spectra of representative diisopropylphenoxide complexes in the solid state and in solution.

$Ln(OAr)_3(THF)_2$ Complexes. Ambient temperature ^1H NMR spectra of the THF bisadducts **4-10** provided varying amounts of information depending upon the paramagnetic influence of the lanthanide metal centers. The ^1H spectra of the THF bisadducts of Nd (**4**), Sm (**5**), Lu (**7**), Pr (**8**), and Yb (**10**) displayed varying degrees of line broadening (Yb > Pr > Nd > Sm > Lu) but were sufficiently well-resolved to show only one type of aryloxide and one type of THF ligand bound to the metal center. Line widths displayed in the ^1H NMR spectra of the Er (**6**) and Gd (**9**) complexes were too broad to be of diagnostic value.

Infrared Spectroscopic Studies. The infrared spectra of $Ln_2(OAr)_6$ compounds exhibit some rather unusual behavior in the ν(C=C) stretching region of the spectra and provide a great deal of insight into the structure of these compounds in solution. Figure 3 and Table 10 show comparisons of this important ν(C=C) region for a number of key compounds reported in this work. The infrared spectra (KBr plates, Nujol mull) of the π-arene-bridged dimeric complexes $Ln_2(OAr)_6$ show *two* distinct ν(C=C) stretching modes in the aromatic region (1588 and 1571 cm^{-1} for Nd (**1**); 1586 and 1572 cm^{-1} for Sm (**2**); 1590 and 1571 cm^{-1} for Er (**3**)) consistent with two significantly different arene environments in the solid state (Figure 3). A similar feature was observed in the solid state infrared spectrum of the uranium analog $U_2(O\text{-}2,6\text{-}i\text{-}Pr_2C_6H_3)_6$ (**11**), which revealed ν(C=C) stretching bands at 1588 and 1553 cm^{-1}.[32] The solution IR spectra of **1-3** (benzene solution) also display *two* distinct ν(C=C) stretching modes in the aromatic region (1590 and 1572 cm^{-1} for Nd (**1**); 1589 and 1572 cm^{-1} for Sm (**2**); 1589 and 1572 cm^{-1} for Er (**3**)); see Figure 3. The close agreement in these values of ν(C=C) stretching modes in both solid state and solution IR spectra of **1-3** strongly

Table 9. Summary of Bond Lengths (Å) and Angles (deg) for $Ln(O\text{-}2,6\text{-}i\text{-}Pr_2C_6H_3)_3(THF)_2$ Molecules

	Ln–O		Ln–O–C		Ln–O(THF)	
$Pr(OAr)_3(THF)_2$	Pr(1)–O(1)	2.142(8)	Pr(1)–O(1)–C(1)	150.9(8)	Pr(1)–O(4)	2.460(8)
	Pr(1)–O(2)	2.158(9)	Pr(1)–O(2)–C(13)	174.2(7)	Pr(1)–O(5)	2.503(9)
	Pr(1)–O(3)	2.216(9)	Pr(1)–O(3)–C(25)	172.7(7)		
$Gd(OAr)_3(THF)_2$	Gd(1)–O(1)	2.138(9)	Gd(1)–O(1)–C(1)	152.8(10)	Gd(1)–O(4)	2.439(9)
	Gd(1)–O(2)	2.156(11)	Gd(1)–O(2)–C(13)	172.6(7)	Gd(1)–O(5)	2.349(10)
	Gd(1)–O(3)	2.096(9)	Gd(1)–O(3)–C(25)	176.1(7)		
$Er(OAr)_3(THF)_2$	Er(1)–O(3)	2.072(10)	Er(1)–O(3)–C(25)	175.0(9)	Er(1)–O(5)	2.344(11)
	Er(1)–O(2)	2.073(10)	Er(1)–O(2)–C(13)	173.0(9)	Er(1)–O(4)	2.348(10)
	Er(1)–O(1)	2.090(10)	Er(1)–O(1)–C(1)	150.7(9)		
$Lu(OAr)_3(THF)_2$	Lu(1)–O(1)	2.041(4)	Lu(1)–O(1)–C(1)	174.2(3)	Lu(1)–O(4)	2.295(3)
	Lu(1)–O(2)	2.048(4)	Lu(1)–O(2)–C(13)	174.3(3)	Lu(1)–O(5)	2.297(4)
	Lu(1)–O(3)	2.042(3)	Lu(1)–O(3)–C(25)	153.0(4)		

Table 10. Infrared Vibration Frequencies (cm^{-1}) for the $\nu(C{=}C)$ Stretch in 2,6-Diisopropylphenoxide Complexes[a]

compd	$\nu(C{=}C)$		medium	ref
$Sm_2(OAr)_6$	1586	1572	Nujol	this work
$Sm_2(OAr)_6$	1589	1572	benzene	this work
$Nd_2(OAr)_6$	1588	1571	Nujol	this work
$Nd_2(OAr)_6$	1590	1572	benzene	this work
$Er_2(OAr)_6$	1590	1571	Nujol	this work
$Er_2(OAr)_6$	1589	1572	benzene	this work
$U_2(OAr)_6$	1588	1553	Nujol	32
$U(OAr')_3$	1583		Nujol	32
$Pr(OAr)_3(THF)_2$	1584		Nujol	this work
$Sm(OAr)_3(THF)_2$	1585		Nujol	this work
$Gd(OAr)_3(THF)_2$	1585		Nujol	this work
$Er(OAr)_3(THF)_2$	1586		Nujol	this work
$Nd(OAr)_3(THF)_2$	1585		Nujol	this work
$Yb(OAr)_3(THF)_2$	1586		Nujol	this work
$Lu(OAr)_3(THF)_2$	1586		Nujol	this work
Li(OAr)	1584		Nujol	this work
HOAr	1585		neat	this work

[a] Ar = 2,6-diisopropylphenoxide; Ar′ = 2,6-di-*tert*-butylphenoxide.

suggest that the solid state η^6-arene-bridged structure is maintained in solution. Although a dimeric structure which involved aryloxide ligands bridging through oxygen would also possess two types of aryloxide ligand (**V**), the C=C stretching frequencies would be expected to be so similar that they may not be resolved as two distinct bands [for example, only one $\nu(C{=}C)$ stretching band is seen at 1590 cm^{-1} for the oxygen-bridged dimer $Y_2(O\text{-}2,6\text{-}Me_2C_6H_3)_6(THF)_2$ or at 1580 cm^{-1} for the monomeric trisolvate $Y(O\text{-}2,6\text{-}Me_2C_6H_3)_3(THF)_3$ and $NaO\text{-}2,6\text{-}Me_2C_6H_3$].[24]

A more detailed examination of the $\nu(C{=}C)$ stretching region reveals that the higher frequency band has an intensity approximately twice that of the lower frequency band, and this is readily seen in Figure 3 for $Sm_2(OAr)_6$. We therefore tentatively assign the higher frequency band to the terminal aryloxide ligands, while the bridging aryloxide is assigned as the source of the lower frequency band. This assignment of stretching modes is consistent with the notion that π-donation from the aromatic ring to the lanthanide metal center will lower the C—C bond order and produce a lower stretching frequency. Further evidence in support of these IR assignments for **1–3** is provided by a comparison of the $\nu(C{=}C)$ stretching bands observed for related diisopropylphenoxide complexes. Table 10 compares the $\nu(C{=}C)$ stretching vibrations in π-arene-bridged $Ln_2(O\text{-}2,6\text{-}i\text{-}Pr_2C_6H_3)_6$ and $U_2(O\text{-}2,6\text{-}i\text{-}Pr_2C_6H_3)_6$ complexes with monomeric $Ln(O\text{-}2,6\text{-}i\text{-}Pr_2C_6H_3)_3(THF)_2$ (Ln = Nd, Pr, Sm, Gd, Er, Yb, Lu), the free alcohol $HO\text{-}2,6\text{-}i\text{-}Pr_2C_6H_3$, the lithium salt $LiO\text{-}2,6\text{-}i\text{-}Pr_2C_6H_3$, and monomeric $U(O\text{-}2,6\text{-}t\text{-}Bu_2C_6H_3)_3$.[32] It can be seen that all species that contain only terminal aryloxide ligands exhibit only one $\nu(C{=}C)$ stretching frequency in a very narrow range 1583–1586 cm^{-1}. Only in the case of the solid state and solution IR spectra of the π-arene-bridged complexes **1-3** and **11** (Table 10) can a second, lower frequency band be observed in the region 1571–1572 cm^{-1} (Ln) or 1553 cm^{-1} (U), consistent with the presence of a second, significantly different type of aryloxide ligand environment. Figure 3 compares the infrared spectra (in the range 1480–1620 cm^{-1}) of **2**, both in the solid state and in solution, with those of the THF adduct $Sm(O\text{-}2,6\text{-}i\text{-}Pr_2C_6H_3)_3(THF)_2$ (**5**) and lithium 2,6-diisopropylphenoxide. It can clearly be seen that the two lower spectra, containing bands for only terminal aryloxide ligands, do not show a lower energy stretching band in the region of 1572 cm^{-1}.

Comparison of the stretching frequency of the lower energy band (1571 cm^{-1} (**1**), 1572 cm^{-1} (**2**), 1572 cm^{-1} (**3**)) with that of the corresponding band in the uranium analog **11** (1553 cm^{-1}) suggests that the uranium–π-arene interaction is slightly stronger than the lanthanide–arene interactions. This proposal is supported by the fact that the average U–C distances (2.92(2) Å) are significantly shorter than the Ln–C distances observed in either **1** (3.035 Å average) or **2** (2.986 and 3.016 Å average) despite the fact that the U(III) metal center is larger than those of Nd(III) and Sm(III) (U(III) 1.025 Å, Nd(III) 0.983 Å, Sm(III) 0.958 Å).[57]

Concluding Remarks

It is well-established that the oligomerization and solution properties in alkoxide complexes of scandium, yttrium, and the lanthanides are highly dependent on the steric requirements of the ligand substituents. In this report we have demonstrated that trivalent neodymium, samarium, and erbium 2,6-diisopropylphenoxide complexes exhibit solid state structural properties similar to those of the uranium analog in the formation of rather unusual dimeric, π-arene-bridged complexes.

Both NMR and IR data for $Ln_2(OAr)_6$ complexes **1** (Nd), **2** (Sm), and **3** (Er) are consistent with the retention of the π-arene bridges in solution, and the infrared spectra are particularly informative with respect to the structure of these complexes in solution. The tendency to retain a π-arene bridge instead of forming the more conventional oxygen-bridged configuration raises some interesting questions regarding the solution behavior of the $U_2(OAr)_6$ analog. Steric interactions between the bulky 2,6-diisopropylphenoxide ligands in the $Ln_2(OAr)_6$ complexes apparently favor the π-arene-bridged structure (**IV**) and preclude adoption of the presumably more stable edge-shared tetrahedral dimer configuration (**V**). The primary steric interaction in **V** should occur between the isopropyl methyl groups on the bridging and terminal aryloxide ligands. The π-arene bridges in the lanthanide dimers, however, are accompanied by very large metal–metal separations of 5.1–5.5 Å, which effectively remove unfavorable interligand interactions. One can draw an analogy here between our lanthanide aryloxide result and some recent observations in the chemistry of transition metal arylimido complexes employing the related (2,6-diisopropylphenyl)imido ligand. When the bulky (2,6-diisopropylphenyl)imido ligand was studied, Bryan and co-workers observed the formation of a novel unbridged ethane-like structure of general formula $M_2(NAr)_6$

(57) Shannon, R. D. *Acta Crystallogr., Sect. A* **1976**, *32*, 751.

where M = Tc and Re.[58] However, upon a decrease in the streric bulk to the (2,6-dimethylphenyl)imido ligand, an edge-bridged tetrahedral dimer of formula $M_2(\mu\text{-NAr})_2(NAr')_4$ was found.[58]

Thus the 2,6-diisopropylphenoxide ligand appears to fill a unique position in lanthanide aryloxide chemistry with respect to steric bulk. While being sufficiently bulky to prevent oligomerization through the agency of Ln–O–Ln bridges, we find that this ligand is small enough to allow the formation of a range of structurally diverse complexes of the types $Ln(OAr)_3(THF)_2$, $Ln(OAr)_3(py)_3$,[33b] K[Ln(OAr)$_4$], K[Ln(OAr)$_4$py],[33b] and $[(ArO)_2Ln(\mu\text{-}\eta\text{-OAr})_2Ln(OAr)_2]$. Efforts are underway to further investigate the extent of π-arene bridges in lanthanide and actinide chemistry, as well as to further delineate the solution and structural chemistry of this fascinating class of compounds.

Experimental Section

General Procedures and Techniques. All manipulations were carried out under an inert atmosphere of oxygen-free UHP grade argon using standard Schlenk techniques or under oxygen-free helium in a Vacuum Atmospheres glovebox. Anhydrous lanthanide trichlorides were purchased from Aldrich (La, Nd) or Strem (Pr, Sm, Gd, Er, Yb, Lu) and used as received. 2,6-Diisopropylphenol was purchased from Aldrich and degassed before use. Potassium 2,6-diisopropylphenoxide was prepared by the reaction of potassium hydride (Aldrich) with 2,6-diisopropylphenol in THF. The compounds $Ln[N(SiMe_3)_2]_3$ (Ln = Nd, Sm, Er, Lu) were prepared by stirring or refluxing the appropriate lanthanide trichloride with 3 equiv of potassium or sodium bis(trimethylsilyl)amide in THF, followed by crystallization from hexane.[59] Solvents were degassed and distilled from Na–K alloy under nitrogen. Benzene-d_6 and toluene-d_8 were degassed, dried over Na–K alloy, and then trap-to-trap-distilled before use. Solvents were taken into the glovebox, and a small amount of each was tested with a solution of sodium benzophenone in THF. Solvents that failed to maintain a purple coloration from this test were not used.

NMR spectra were recorded at 22 °C on a Bruker AF 250 or at 17 °C on a Varian Unity 300 spectrometer in benzene-d_6 or toluene-d_8. All ^{1}H NMR chemical shifts are reported in ppm relative to the ^{1}H impurity in benzene-d_6 or toluene-d_8 set at δ 7.15 or 2.09, respectively. NMR spectra of paramagnetic lanthanide species are highly temperature dependent; thus it is important to note that the temperatures quoted represent average room temperatures and are approximate values. Infrared spectra were recorded on a Digilab FTS-40 spectrometer. Solid state spectra were taken as Nujol mulls between KBr plates, while solution spectra were recorded in benzene solution versus a solvent blank in KBr cells. Elemental analyses were performed on a Perkin-Elmer 2400 CHN analyzer. Elemental analysis samples were prepared and sealed in tin capsules in the glovebox prior to combustion.

$Nd_2(O\text{-}2,6\text{-}i\text{-}Pr_2C_6H_3)_6$ (1). A 5.00-g (7.98 mmol) sample of $Nd[N(SiMe_3)_2]_3$ was dissolved in 150 mL of toluene in a 250-mL Schlenk reaction vessel, and then 4.20 mL (22.66 mmol) of 2,6-diisopropylphenol was added. The reaction vessel was fitted with a reflux condenser and the mixture refluxed under argon for 2 h before being returned to the drybox. The color of the solution had changed from pale blue to pale blue/green. The solution was filtered through Celite, and its volume was reduced to 50 mL before being placed at –40 °C. Over a period of 2 days, pale blue crystals were deposited. These were isolated by decantation and allowed to dry. A second crop of crystals was isolated by concentration of the filtrate and cooling again to –40 °C. Total yield: 4.01 g (79%). ^{1}H NMR (250 MHz, C_6D_6, 23 °C): δ 40.62 (br s, 2 H, C*H*Me$_2$), 13.23 (s, 4 H, OAr *meta*), 10.28 (s, 2 H, OAr *para*), 8.18 (br m, 4 H, C*H*Me$_2$), 4.48 (br s, 12 H, CH*Me$_2$*), –0.82 (br s, 24 H, CH*Me$_2$*), –20.25 (br s, 2 H, OAr *meta*), –44.41 (br s, 1 H, OAr *para*). IR (KBr, Nujol, cm^{-1}): 1588 (m), 1571 (m), 1432 (s), 1355 (m), 1324 (s), 1294 (w), 1260 (s), 1202 (s), 1110 (m), 1096 (m), 1039 (m), 932 (w), 887 (s), 857 (s), 806 (m), 777 (m), 752 (s), 693 (m), 684 (sh, m), 570 (m), 551 (m). IR (C_6H_6, cm^{-1}): 1590 (w), 1572 (w), 1450 (m), 1427 (s), 1380 (w), 1367 (w), 1355 (m), 1326 (s), 1292 (w), 1265 (s), 1205 (m), 1112 (w), 1095 (w), 1060 (vw), 935 (w), 888 (m), 860 (m), 836 (w), 804 (w), 792 (vw), 776 (w), 751 (m), 568 (w), 551 (vw). Anal. Calcd for $C_{72}H_{102}Nd_2O_6$: C, 63.96; H, 7.60; N, 0.00. Found: C, 63.31; H, 7.29; N, 0.07.

$Sm_2(O\text{-}2,6\text{-}i\text{-}Pr_2C_6H_3)_6$ (2). A 2.00-g (3.17 mmol) sample of $Sm[N(SiMe_3)_2]_3$ was dissolved in 100 mL of toluene in a 250-mL Schlenk reaction vessel, and then a solution of 1.11 g (9.55 mmol) of 2,6-diisopropylphenol in 10 mL of toluene was added to give a deep yellow solution. The reaction vessel was fitted with a reflux condenser and the mixture refluxed for 2 h before being returned to the drybox. The solution was filtered through Celite, and its volume was reduced to 20 mL before being placed at –40 °C. Over a period of 2 days, deep yellow crystals were deposited. These were isolated by decantation and allowed to dry. Yield: 1.95 g (90%). ^{1}H NMR (250 MHz, C_6D_6, 23 °C): δ 11.81 (br s, 2 H, C*H*Me$_2$), 10.28 (s, 2 H, OAr *para*), 7.97 (s, 4 H, OAr *meta*), 4.21 (br m, 4 H, C*H*Me$_2$), 2.31 (br s, 2 H, OAr *meta*), 1.74 (br s, 12 H, CH*Me$_2$*), 1.02 (br s, 24 H, CH*Me$_2$*), –3.10 (br s, 1 H, OAr *para*). ^{13}C NMR (C_6D_6, 62.5 MHz, 22 °C): δ 23.5 (q, J_{C-H} = 126 Hz, CH*Me$_2$*), 23.6 (q, J_{C-H} = 123 Hz, CH*Me$_2$*), 30.6 (d, J_{C-H} = 125 Hz, *C*HMe$_2$), 32.8 (d, J_{C-H} = 127 Hz, *C*HMe$_2$), 90.0 (d, J_{C-H} = 157 Hz, OAr *para*), 111.7 (d, J_{C-H} = 160 Hz, OAr *para*), 119.2 (d, J_{C-H} = 159 Hz, OAr *meta*), 125.3 (d, J_{C-H} = 150 Hz, OAr *meta*), 136.2 (s, OAr *ortho*), 136.8 (s, OAr *ortho*), 162.3 (s, OAr *ipso*), 164.8 (s, OAr *ipso*). IR (Nujol, cm^{-1}): 1586 (m), 1572 (m), 1430 (s), 1381 (m), 1359 (m), 1326 (s), 1294 (m), 1263 (s), 1205 (s), 1110 (m), 1097 (m), 1040 (m), 1021 (w), 933 (w), 887 (s), 858 (s), 808 (m), 777 (s), 753 (s), 695 (s), 573 (m), 553 (m). IR (Benzene, cm^{-1}): 1589 (w), 1572 (w), 1450 (m), 1429 (s), 1380 (w), 1367 (w), 1351 (m), 1326 (s), 1292 (w), 1266 (s), 1205 (m), 1110 (w), 1094 (w), 1061 (vw), 935 (w), 887 (m), 860 (w), 805 (w), 793 (vw), 774 (w), 750 (m), 572 (w), 553 (vw). Anal. Calcd for $C_{72}H_{102}Sm_2O_6$: C, 63.38; H, 7.54; N, 0.00. Found: C, 62.46; H, 7.18; N, 0.00.

$Er_2(O\text{-}2,6\text{-}i\text{-}Pr_2C_6H_3)_6$ (3). A 1.578-g (2.29-mmol) sample of $Er[N(SiMe_3)_2]_3$ was dissolved in 75 mL of toluene in a 250-mL Schlenk reaction vessel, and then 1.225 mL (6.87 mmol) of 2,6-diisopropylphenol was added. The resulting pink solution was stirred at room temperature for 4$^1/_2$ days. The solution was filtered through Celite and the solvent removed in vacuo. The solid was washed with hexane to remove any excess $Er[N(SiMe_3)_2]_3$. The remaining solid was dissolved in toluene, and the solution was placed at –15 °C. Over a period of 2 weeks, a pink semicrystalline solid was deposited. This solid was isolated by decantation and allowed to dry. A second crop of crystals was isolated by concentration of the filtrate and cooling again to –40 °C. Total yield: 0.470 g (29%). ^{1}H NMR (300 MHz, C_6D_6, 23 °C): broad resonances seen at δ –7.8, –16.9, –17.2, –23.1. IR (KBr, Nujol, cm^{-1}): 1590 (m), 1571 (m). IR (C_6H_6, cm^{-1}): 1589 (w), 1572 (w), 1453 (m), 1430 (s), 1380 (w), 1357 (m), 1331 (s), 1297 (w), 1265 (s), 1206 (m), 1111 (w), 1098 (w), 935 (w), 887 (m), 863 (m), 810 (w), 793 (vw), 775 (w), 751 (m). Anal. Calcd for $C_{72}H_{102}Er_2O_6$: C, 61.85; H, 7.35; N, 0.00. Found: C, 61.65; H, 7.80; N, 0.31.

$Nd(O\text{-}2,6\text{-}i\text{-}Pr_2C_6H_3)_3(THF)_2$ (4). A sample of $Nd_2(O\text{-}2,6\text{-}i\text{-}Pr_2C_6H_3)_6$ (1) (0.518 g, 0.38 mmol) was placed in a 50-mL flask, and 20 mL of THF was added. After 5 min of stirring, the THF was removed in vacuo to leave a pale blue microcrystalline solid identified as $Nd(O\text{-}2,6\text{-}i\text{-}Pr_2C_6H_3)_3(THF)_2$ (0.553 g, 88%). ^{1}H NMR (250 MHz, C_6D_6): δ 18.38 (br s, 6 H, C*H*Me$_2$), 14.82 (s, 6 H, OAr *meta*), 11.87 (s, 3 H, OAr *para*), 3.89 (br s, 36 H, CH*Me$_2$*), –15.55 (br s, 8 H, THF β), –27.43 (br s, 8 H, THF α). IR (Nujol, cm^{-1}): 1585 (m), 1426 (s), 1356 (m), 1327 (s), 1263 (s), 1204 (s), 1109 (m), 1094 (m), 1053 (w), 1042 (m), 1018 (s), 933 (m), 916 (w), 884 (s), 856 (s), 803 (w), 796 (w), 754 (s), 722 (sh, w), 687 (s), 561 (s), 547 (sh, w), 417 (w), 409 (w). Anal. Calcd for $C_{44}H_{67}O_5Nd$: C, 64.43; H, 8.23; N, 0.00. Found: C, 64.05; H, 8.16; N, 0.02.

$Sm(O\text{-}2,6\text{-}i\text{-}Pr_2C_6H_3)_3(THF)_2$ (5). A THF solution (125 mL) of potassium diisopropylphenoxide was prepared by reacting 1.41 g (35.2 mmol) of potassium hydride with 6.25 g (35.0 mmol) of 2,6-diisopropylphenoxide and filtering the solution through a Celite pad. To the filtrate was added 3.00 g (11.7 mmol) of samarium trichloride, and the solution was stirred for 2 days. The solvent was removed in vacuo, the solid was extracted with toluene (100 mL), and the extract was filtered through a Celite pad. The resulting yellow filtrate was concentrated to approximately 65 mL and placed at –40 °C (at which point a pale solid was already coming out of solution). After 2 days, a pale crystalline solid was isolated by decanting the mother liquor and allowing the solid to dry in the drybox. A second crop was obtained by concentration of the mother liquor and placing at –40 °C. The yellow solid was isolated as above. Total yield: 4.79 g (50%). ^{1}H NMR (250 MHz, C_6D_6): δ 7.79 (d, J = 7 Hz, 6 H, OAr *meta*), 7.55 (t, J = 7 Hz, 3 H, OAr *para*), 5.20 (septet, J = 7 Hz, 6 H, C*H*Me$_2$), 1.69 (d, J = 7 Hz, 36 H, CH*Me$_2$*), –0.01 (br

(58) Burrell, A. K.; Clark, D. L.; Gordon, P. L.; Sattelberger, A. P.; Bryan, J. C. *J. Am. Chem. Soc.*, in press.
(59) (a) Bradley, D. C.; Ghotra, J. S.; Hart, F. A. *J. Chem. Soc., Dalton Trans.* **1973**, 1021. (b) Evans, W. J.; Golden, R. E.; Ziller, J. W. *Inorg. Chem.* **1991**, *30*, 4963.

m, 8 H, THF α), –0.84 (br m, 8 H, THF β). IR (Nujol, cm^{-1}): 1585 (m), 1430 (s), 1358 (m), 1329 (s), 1267 (s), 1208 (s), 1159 (w), 1110 (m), 1096 (m), 1056 (w), 1044 (m), 1018 (s), 955 (w), 935 (m), 885 (s), 859 (s), 803 (w), 797 (w), 754 (s), 687 (s), 573 (sh, w), 561 (s), 548 (sh, w). Anal. Calcd for $C_{44}H_{67}O_5Sm$: C, 63.95; H, 8.17; N, 0.00. Found: C, 63.09; H, 6.68; N, 0.04.

Er(O-2,6-*i*-Pr$_2$C$_6$H$_3$)$_3$(THF)$_2$ (6). A sample of Er$_2$(O-2,6-*i*-Pr$_2$C$_6$H$_3$)$_6$ (3) (0.271 g, 0.19 mmol) was placed in a 50-mL flask, and 20 mL of THF was added. After 5 min of stirring, the THF was removed in vacuo to leave a pink microcrystalline solid identified as Er(O-2,6-*i*-Pr$_2$C$_6$H$_3$)$_3$(THF)$_2$ (0.290 g, 89%). ^{1}H NMR (250 MHz, C_6D_6): broad resonances observed at δ 91.6, –17.0, –22.9, –77.7 (peak width at half-height 100–750 Hz). IR (Nujol, cm^{-1}): 1586 (m), 1431 (s), 1366 (w), 1357 (m), 1303 (w), 1295 (w), 1273 (s), 1265 (s), 1209 (m), 1172 (w), 1151 (w), 1141 (w), 1108 (w), 1095 (w), 1058 (w), 1042 (m), 1014 (m), 954 (w), 933 (w), 925 (w), 916 (w), 900 (w), 888 (s), 863 (s), 804 (w), 795 (w), 757 (s), 752 (s), 691 (m), 572 (w), 566 (w). Anal. Calcd for $C_{44}H_{67}ErO_5$: C, 62.67; H, 8.01. Found: C, 62.76; H, 7.55.

Lu(O-2,6-*i*-Pr$_2$C$_6$H$_3$)$_3$(THF)$_2$ (7). To a solution of 0.50 g (0.76 mmol) of Lu[N(SiMe$_3$)$_2$]$_3$ in 100 mL of toluene in a 250-mL Schlenk vessel was added a solution of 0.40 g (2.24 mmol) of 2,6-diisopropylphenol in 10 mL of toluene. The flask was attached to a reflux condenser and the solution refluxed for 1 h before being returned to the drybox. A 1-mL portion of THF was then added, and the solution was allowed to stir for 30 min. The volume of the pale green solution was reduced in vacuo to 20 mL and placed at –40 °C. Pale green crystals were deposited over a period of 2 days. These were decanted free from solvent and allowed to dry in the box atmosphere. Yield: 0.49 g (76%). ^{1}H NMR (250 MHz, C_6D_6): δ 7.22 (d, *J* = 8 Hz, 6 H, OAr *meta*), 6.96 (t, *J* = 8 Hz, 3 H, OAr *para*), 3.80 (m, 8 H, THF α), 3.54 (septet, *J* = 7 Hz, 6 H, C*H*Me$_2$), 1.31 (d, *J* = 7 Hz, 36 H, CH*Me*$_2$), 1.06 (m, 8 H, THF β). IR (Nujol, cm^{-1}): 1586 (m), 1432 (s), 1367 (m), 1357 (m), 1333 (s), 1304 (w), 1296 (w), 1274 (s), 1264 (sh, s), 1209 (m), 1171 (w), 1160 (w), 1140 (w), 1108 (w), 1095 (w), 1058 (w), 1042 (m), 1015 (m), 954 (w), 934 (w), 916 (w), 888 (s), 862 (s), 803 (w), 794 (w), 757 (s), 752 (s), 691 (m), 571 (w), 563 (w). Anal. Calcd for $C_{44}H_{67}LuO_5$: C, 62.10; H, 7.94. Found: C, 62.01; H, 7.89.

Pr(O-2,6-*i*-Pr$_2$C$_6$H$_3$)$_3$(THF)$_2$ (8). To a vigorously stirred suspension of 2.00 g (8.09 mmol) of praseodymium trichloride in 100 mL of THF was added a solution of 5.25 g (24.26 mmol) of potassium 2,6-diisopropylphenoxide in 100 mL of THF. The mixture was stirred at room temperature for 4 days to produce a pale brown suspension. The suspension was filtered through Celite to give a clear brown filtrate, and all solvent was then removed in vacuo to leave a brown solid. The solid was dissolved in 75 mL of toluene, and the solution was filtered through Celite. The filtrate, was reduced to 50 mL in volume, was then allowed to stand and slowly evaporate in the box. After 2 days, a mass of brown crystals had been deposited. These were collected on a frit, washed with hexane, and allowed to dry in the box atmosphere. Yield: 1.42 g (20%). ^{1}H NMR (250 MHz, toluene-d_8): δ 24.02 (br s, 6 H, C*H*Me$_2$), 19.11 (s, 6 H, OAr *meta*), 15.61 (s, 3 H, OAr *para*), 4.58 (br s, 36 H, CH*Me*$_2$), –26.78 (br m, 8 H, THF β), –43.10 (v br m, 8 H, THF α). IR (Nujol, cm^{-1}): 1584 (m), 1430 (s), 1357 (m), 1328 (s), 1264 (s), 1206 (s), 1157 (w), 1138 (w), 1109 (m), 1095 (m), 1056 (w), 1040 (m), 1020 (s), 954 (w), 932 (w), 916 (w), 885 (s), 856 (s), 803 (w), 793 (w), 757 (s), 752 (s), 685 (s), 615 (w), 605 (w), 556 (m). Anal. Calcd for $C_{44}H_{67}O_5Pr$: C, 64.69; H, 8.27. Found: C, 64.39; H, 7.56.

Gd(O-2,6-*i*-Pr$_2$C$_6$H$_3$)$_3$(THF)$_2$ (9). To a vigorously stirred slurry of 2.469 g (9.37 mmol) of gadolinium trichloride in 75 mL of THF was added a solution of 6.08 g (28.10 mmol) of potassium 2,6-diisopropylphenoxide in 100 mL of THF. The mixture was allowed to stir at room temperature for 48 h and then filtered through Celite to give a clear, pale yellow filtrate. All solvent was removed from the filtrate in vacuo to leave a yellow solid residue, which was extracted into 75 mL of warm toluene. The extract was then filtered through Celite, the volume of the filtrate was reduced to 50 mL, and this solution was placed in the freezer at –40 °C. A mass of pale yellow crystals was deposited in the flask over a period of 3 days. The crystals were decanted free from residual solvent and allowed to dry under a helium atmosphere. Yield: 4.555 g (58%). ^{1}H NMR (250 MHz, C_6D_6): only two very broad humps seen at δ 9.0, 3.5. IR (Nujol, cm^{-1}): 1585 (m), 1427 (s), 1357 (m), 1331 (s), 1267 (s), 1207 (s), 1176 (w), 1157 (w), 1139 (w), 1109 (m), 1094 (m), 1059 (w), 1040 (s), 1015 (s), 952 (w), 934 (w), 885 (s), 860 (s), 804 (w), 794 (w), 757 (s), 752 (s), 688 (s), 562 (m). Anal. Calcd for $C_{44}H_{67}GdO_5$: C, 63.42; H, 8.10. Found: C, 63.09; H, 7.19.

Yb(O-2,6-*i*-Pr$_2$C$_6$H$_3$)$_3$(THF)$_2$ (10). To a vigorously stirred slurry of 2.50 g (8.95 mmol) of ytterbium trichloride in 75 mL of THF was added a solution of 5.81 g (26.85 mmol) of potassium 2,6-diisopropylphenoxide in 100 mL of THF. The mixture was allowed to stir at room temperature for 48 h and then filtered through Celite to give a clear yellow filtrate. All solvent was removed from the filtrate in vacuo to leave a pale yellow solid residue, which was extracted into 100 mL of warm toluene. The extract was then filtered through Celite, the volume of the filtrate was reduced to 75 mL, and this solution was placed in a freezer at –40 °C. A mass of yellow crystals was deposited in the flask over a period of 3 days. The crystals were decanted free from residual solvent and allowed to dry in the box atmosphere. Yield: 5.14 g (68%). ^{1}H NMR (250 MHz, C_6D_6): δ 153.24 (br m, 8 H, THF α), 79.27 (br m, 8 H, THF β), 9.77 (s, 3 H, OAr *para*), –13.39 (s, 6 H, OAr *meta*), –15.56 (br s, 36 H, CH*Me*$_2$), –16.78 (br m, *J* = 7 Hz, 6 H, C*H*Me$_2$). IR (Nujol, cm^{-1}): 1586 (m), 1433 (s), 1357 (m), 1331 (s), 1273 (s), 1210 (m), 1171 (w), 1156 (w), 1109 (w), 1093 (w), 1041 (m), 1015 (m), 954 (w), 934 (w), 888 (s), 863 (s), 804 (w), 794 (w), 756 (s), 751 (s), 692 (m), 572 (m). Anal. Calcd for $C_{44}H_{67}YbO_5$: C, 62.24; H, 7.95. Found: C, 61.67; H, 7.71.

Crystallographic Studies. Nd$_2$(O-2,6-*i*-Pr$_2$C$_6$H$_3$)$_6$ (1). Crystal data and data collection and processing parameters are given in Table 1. General operating procedures have been described elsewhere.[60] The diffractometer utilized for data collection for **1** was designed and constructed locally at the IUMSC. The diffractometer consisted of a Picker four-circle goniostat equipped with a Furnas monochromator (HOG crystal) and Picker X-ray generator interfaced to a Z80 microprocessor and controlled by an RS232 Serial port on an IBM PC microcomputer. Motors were Slo-Syn stepping motors, and a special top/bottom–left/right slit assembly was used to align the crystal. All computations were performed on IBM-compatible microcomputer systems. A suitable fragment of a larger clump of crystals was affixed to a glass fiber using silicone grease and transferred to the goniostat, where it was cooled to –162 °C for characterization and data collection. All handling was performed using standard inert atmosphere handling techniques. A systematic search of a limited hemisphere of reciprocal space located a set of diffraction maxima with symmetry and systematic absences corresponding to the unique monoclinic space group $P2_1/a$. Subsequent solution and refinement confirmed this choice.

Data were collected using a standard moving crystal–moving detector technique with fixed background counts at each extreme of the scan. Data were corrected for Lorentz and polarization effects and equivalent data averaged. The structure was solved by direct methods (MULTAN78) and Fourier techniques and refined by full-matrix least-squares techniques. In general, the data were not sufficiently good to locate the hydrogen atom positions, so all hydrogens were introduced in fixed idealized positions for the final cycles of refinement. A final difference Fourier map was featureless, the largest peaks being 0.88 e Å^{-3}.

Sm$_2$(O-2,6-*i*-Pr$_2$C$_6$H$_3$)$_6$ (2). The yellow platelike crystals were examined in mineral oil under an argon stream. A crystal measuring 0.2 × 0.15 × 0.13 mm was selected, affixed to a glass fiber using Apiezon grease, and transferred to the –70 °C nitrogen coldstream of an Enraf-Nonius CAD4 diffractometer with graphite-monochromated Mo Kα radiation. Unit cell parameters were determined from the least-squares refinement of $[(\sin(\theta)/\lambda)]^2$ values for 24 accurately centered reflections. Two reflections were chosen as intensity standards and were measured every 7200 s of X-ray exposure time, and three orientation controls were measured every 250 reflections.

The intensities were corrected for Lorentz and polarization effects, and an empirical absorption correction based on azimuthal scans was applied. Equivalent reflections were merged (R_{int} = 0.0165), and systematically absent reflections were rejected. The structure was solved by routine Patterson and Fourier methods and refined using full-matrix least-squares techniques. After inclusion of anisotropic thermal parameters for all non-hydrogen atoms and geometrical generation of hydrogen atoms, which were constrained to "ride" upon the appropriate carbon atoms, final refinement using 6789 unique observed $[F > 4\sigma(F)]$ reflections converged at $R = 0.045$, $R_w = 0.064$ {where $w = [\sigma^2(F) + 0.0006F^2]^{-1}$}. A final difference Fourier map was featureless, with the largest deviations being +0.53 and –0.68 e Å^{-3}. All calculations were performed using the SHELXTL PLUS suite of computer programs (Siemens Analytical X-ray Instruments, Inc., 1990).

Er(O-2,6-*i*-Pr$_2$C$_6$H$_3$)$_3$(THF)$_2$ (6). The crystals consisted of well-formed transparent blocks of a slightly yellow (or pink) tinge. A suitable

(60) Chisholm, M. H.; Folting, K.; Huffman, J. C.; Kirkpatrick, C. C. *Inorg. Chem.* **1984**, *23*, 1021.

crystal was affixed to the end of a glass fiber using silicone grease and transferred to the goniostat, where it was cooled to −170 °C for characterization and data collection. Inert atmosphere handling techniques were used. A systematic search of a limited hemisphere of reciprocal space located a set of diffraction maxima with monoclinic symmetry and extinctions corresponding to either space group $P2_1$ or $P2_1/m$. Subsequent solution and refinement of the structure revealed the noncentrosymmetric space group to be the correct choice.

Data were collected using a moving-crystal, moving-detector technique with fixed backgrounds counts at each extreme of the scan. Data were corrected for Lorentz and polarization effects and equivalent data averaged. The structure was readily solved by direct methods (MULTAN78) and standard Fourier techniques. A difference map phased on the non-hydrogen atoms clearly located the position of most hydrogen atoms, and they were included in the final cycles of refinement as fixed atom contributors.

A final difference Fourier map was essentially featureless with the exception of several peaks of approximate density 0.7 e Å^{-3} in the vicinity of the Er atom.

Lu(O-2,6-*i*-Pr$_2$C$_6$H$_3$)$_3$(THF)$_2$ (7). The crystals were examined in mineral oil under an argon stream, and a suitable crystal measuring 0.25 × 0.25 × 0.25 mm was mounted on a glass fiber with Apiezon grease and transferred to the −70 °C nitrogen coldstream of an Enraf-Nonius CAD4 diffractometer. Twenty-five reflections in a 2θ range 28–36° were used to obtain a monoclinic unit cell, and data were collected in the 2θ range 2–50°. Two reflections were chosen as intensity standards and were measured every 3600 s of X-ray exposure time, and two orientation controls were measured every 250 reflections.

The intensities were corrected for Lorentz and polarization effects, and an empirical absorption correction based on azimuthal scans was applied. The structure was readily solved by Patterson methods and subsequent difference Fourier maps. After inclusion of anisotropic thermal parameters for all non-hydrogen atoms and geometrical generation of hydrogen atoms, which were constrained to "ride" upon the appropriate carbon atoms, final refinement using 4581 unique observed [$F > 4.0\sigma(F)$] reflections converged at $R = 0.021$, $R_w = 0.031$ {where $w = [\sigma^2(F) + 0.0006F^2]^{-1}$}. All calculations were performed using the SHELXTL PLUS suite of computer programs (Siemens Analytical X-ray Instruments, Inc., 1990).

Pr(O-2,6-*i*-Pr$_2$C$_6$H$_3$)$_3$(THF)$_2$ (8). The pale brown/green crystals were examined in mineral oil under an argon stream, and a suitable crystal measuring 0.225 × 0.125 × 0.125 mm was mounted on a glass fiber with Apiezon grease and transferred to the −70 °C nitrogen coldstream of an Enraf-Nonius CAD4 diffractometer. Twenty-five carefully centered reflections were used to obtain a monoclinic unit cell, and data were collected in the 2θ range of 2 to 50°. Two reflections were chosen as intensity standards and were measured every 3600 s of X-ray exposure time, and two orientation controls were measured every 250 reflections.

The intensities were corrected for Lorentz and polarization effects, and an empirical absorption correction based on azimuthal scans was applied. The structure was readily solved by Patterson methods and subsequent difference Fourier maps. After inclusion of anisotropic thermal parameters for all non-hydrogen atoms and geometrical generation of hydrogen atoms, which were constrained to "ride" upon the appropriate carbon atoms, final refinement using 3207 unique observed [$F > 4.0\sigma(F)$] reflections converged at $R = 0.045$, $R_w = 0.061$ {where $w = [\sigma^2(F) + 0.0006F^2]^{-1}$}. All calculations were performed using the SHELXTL PLUS suite of computer programs (Siemens Analytical X-ray Instruments, Inc., 1990).

Gd(O-2,6-*i*-Pr$_2$C$_6$H$_3$)$_3$(THF)$_2$ (9). The colorless crystals were examined in mineral oil under an argon stream, and a suitable crystal measuring 0.3 × 0.24 × 0.2 mm was mounted on a glass fiber with Apiezon grease and transferred to the −70 °C nitrogen coldstream of a Siemens R3m/V diffractometer. Fifty carefully centered reflections were used to obtain a monoclinic unit cell, and data were collected in the 2θ range of 2–50°. Two reflections were chosen as intensity standards and were measured every 3600 s of X-ray exposure time, and two orientation controls were measured every 250 reflections.

The intensities were corrected for Lorentz and polarization effects, and an empirical absorption correction based on azimuthal scans was applied. The structure was readily solved by Patterson methods and subsequent difference Fourier maps. After inclusion of anisotropic thermal parameters for all non-hydrogen atoms and geometrical generation of hydrogen atoms, which were constrained to "ride" upon the appropriate carbon atoms, final refinement using 3568 unique observed [$F > 4.0\sigma(F)$] reflections converged at $R = 0.054$, $R_w = 0.073$ {where $w = [\sigma^2(F) + 0.001F^2]^{-1}$}. All calculations were performed using the SHELXTL PLUS suite of computer programs (Siemens Analytical X-ray Instruments, Inc., 1990).

Acknowledgment. We thank Drs. A. P. Sattelberger and R. A. Andersen for helpful discussions. This work was performed under the auspices of the Office of Energy Research, Division of Chemical Sciences, and the Office of Nuclear Material Production, U.S. Department of Energy. Los Alamos National Laboratory is operated by the University of California for the U.S. Department of Energy under Contract W-7405-ENG-36.

Supplementary Material Available: Tables of data collection parameters, fractional coordinates and isotropic thermal parameters, bond distances, bond angles, and anisotropic thermal parameters for **1**, **2**, and **6**–**9** (38 pages). Ordering information is given on any current masthead page.